國立臺灣大學工學院機械工程學研究所

碩士論文

Department of Mechanical Engineering

College of Engineering

National Taiwan University

Master Thesis

結構最佳化之兩點分段適應近似法

Two-Point Piecewise Adaptive Approximation for Structural

Optimization

柯浩宇

Hao-Yu Ke

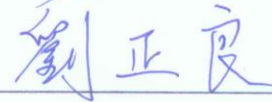指導教授：鍾添東 博士

Advisor: Tien-Tung Chung, Ph.D.

中華民國 105 年 8 月
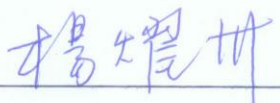
August 2016

國立臺灣大學碩士學位論文
口試委員會審定書

結構最佳化之兩點分段適應近似法
Two-Point Piecewise Adaptive Approximation for Structural Optimization

本論文係柯浩宇君（R03522633）在國立臺灣大學機械工程學系完成之碩士學位論文，於民國 105 年 08 月 01 日承下列考試委員審查通過及口試及格，特此證明

口試委員：

鍾添東	_（簽名）_	（簽名）
（指導教授）		
劉正良		
史建中		

系主任 _____ （簽名）

i

誌謝

　　首先要感謝指導教授鍾添東老師在碩士班兩年來的指導，引領我進入結構最佳化的研究，並在研究過程中給予指導。另外也感謝口試委員史建中教授與劉正良教授的指教與建議，使本文更臻完善。

　　在碩士班的兩年，要感謝電腦輔助設計實驗室的成員，包含同窗尚哲、慶雄、永健、以磬在學習路上的陪伴；以及峰遠、騰輝、維德、期文、承楷、智濠與嘉榮的協助與關心。

　　最後感謝我的父母作為我整個學生生涯最大的後盾，無論是物質上的支援或是對生涯規劃的建議，讓我可以無後顧之憂的完成學業。

中文摘要

　　本研究提出兩點分段適應近似法應用於結構最佳化上。為使數學最佳化理論能與結構設計結合，必須透過近似法將結構之行為諸如應力、位移、頻率等轉換成以設計變數表示的顯函數。最佳解便能透過解決數個由近似函數構成的最佳化問題得到。為確保近似品質，近似函數會考量函數的單調性來建立。由於許多結構行為對設計變數的變化近乎單調函數，兩點分段適應近似法確保建立單調的近似函數以確保近似品質，並在兩點微分值異號時亦能建立非單調函數以符合兩點靈敏度值。並且此近似法採用分段函數解決過往近似法中不當近似的產生。此研究亦整合最佳化程式、CAD 軟體與有限元素分析軟體進行自動化結構最佳設計，並以多個結構最佳化的問題驗證本近似法於結構最佳化的實用性，並另實際應用於電路板等效有限元素模型建立與精密檢測平台的設計之中。

關鍵字：結構最佳化、連續近似最佳化、兩點近似法、有限元素分析、非線性規劃

ABSTRACT
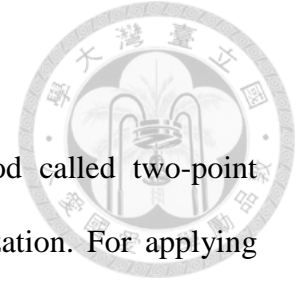
This study proposes a new two-point approximation method called two-point piecewise adaptive approximation (TPPAA) for structural optimization. For applying the mathematical optimization to structural design, several kinds of structural behavior, including stress, displacement and natural frequency, are represented as explicit functions of design variables by approximation technique. The optimum design can be found with sequential sub-problems solved, which is known as sequential approximate optimization (SAO). To ensure the approximation quality, structural behavior is approximated with considering the monotonicity. Monotonic functions are available in TPPAA when the first order derivatives of two successive design points have the same signs since many kinds of structural behavior vary quasi-monotonically with respect to design variables. Non-monotonic form can also be obtained when the two derivatives of two successive design points have different signs. TPPAA adopts the piecewise approximate functions to avoid inappropriate approximation that existing approximation schemes would encounter. In this study, a program integrating ANSYS, AutoCAD and Microsoft Visual C++ is developed for automated structural optimization. The practicability of TPPAA is examined in several structural optimization problems and the comparison of several approximation methods are also presented. Furthermore, TPPAA is applied to optimum design of large structures, such as effective FE model construction of PCB and design of high-accuracy measuring stage structure.

Keyword: Structural optimization, Sequential approximate optimization, Two-point approximation method, Finite element analysis, Nonlinear programming
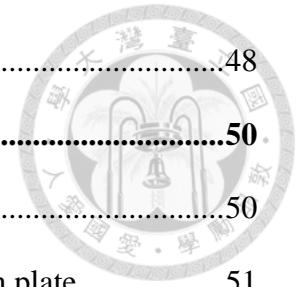
CONTENTS

LIST OF FIGURES

viii

LIST OF TABLES

LIST OF SYMBOLS

E	Elastic modulus
$h(\vec{x})$	Original function to be approximated
$h(\vec{x}_0)$	Function value at the current design point
$h(\vec{x}_1)$	Function value at the previous design point
n	Number of design variables
n_b	Number of behavior constraints
n_c	Number of constraints
n_s	Number of size constraints
x_{0i}	The i-th design variable at the current design point
x_{1i}	The i-th design variable at the previous design point
x_i	The i-th design variable
$\vec{x}$	Design variable vector
$\vec{x}_0$	Design variable vector of the current design point
$\vec{x}_1$	Design variable vector of the previous design point
$x_i^{(k)}$	The i-th design variable in k-th iteration
δ	The given number for criterion of adoption of substitute function
ν	Poisson's ratio
ρ	Density
σ_i	Stress in the i-th element

xiii

Chapter 1　　Introduction
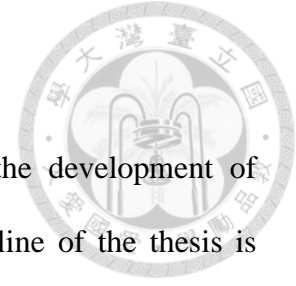
In this chapter, the history of structural optimization and the development of approximation methods are briefly introduced first. Then, the outline of the thesis is presented.

1.1　　Introduction to structural optimization

Structural optimization has been developed more than a century. The main purpose of structural optimization is to improve the design under specific restrictions. Conventionally, design improvement relies on the engineer's experience with trial and error. It costs considerable time and may not obtain the optimal result. Nowadays, automated structural design is available with integrating well developed finite element analysis software and optimization theory. It can find the optimum design with less subjective judgement.

With the development of finite element method, structural analysis is no longer limited to the theoretical derivation. However, it takes considerable time for the large and complicate structures. In order to save the time of design process, approximation technique is introduced.

Approximation methods converts the implicit structural functions into explicit ones to generate the sub-problems, which can be solved with mathematical optimization. It saves much efforts by reducing the number of repeated finite element analyses.

Local approximation schemes construct approximated functions from the response and the sensitivities of a design point. Hence the problem with implicit structural behavior can be transformed into a mathematical problem with explicit functions with the approximation reliable around the design point. After solving sequential sub-problems, the optimal solution can be found after the process converging. This

1

technique is also known as sequential approximate optimization (SAO).

For the less finite element analyses in SAO process, the choice of the approximation scheme is better to depend on the characteristics of the problem. For instance, in simple truss problems with design variables of cross section area, direct linear approximation is the best for total weight of truss, reciprocal approximation is more appropriate for stress and displacement. However, for the complicate cases, it is still hard to determine the most suitable scheme. In spite of that, some principles of approximation may be held to ensure the approximation quality for general cases.
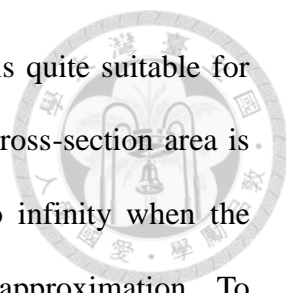
1.2   Paper review

In 1904, Michell calculated the theoretical lower bound of the weight of truss structures with stress constraints [1]. The theoretical derivation of ideal structures was an important inspiration for structural optimization. After finite element method was proposed and developed maturely, structural optimization is valid for designing complicate structures.

In 1974, Schmit and Farshi applied approximation concepts to convert structural behavior into explicit functions of design variables [2]. This method turned limited information from structural analyses into simple approximate functions, and greatly reduced the time of structural optimization process.
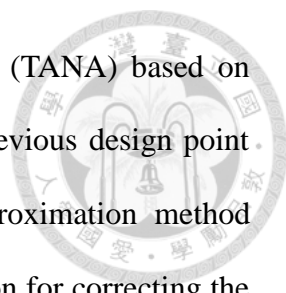
So far, a lot of local approximation methods have been developed. Among these schemes, direct linear approximation is the most fundamental approach which performs the 1st order Taylor series expansion in terms of design variables. However, most structural characteristics are nonlinear, this method may not be reliable for therefore. To enhance the approximation quality, some scholars proposed reciprocal approximation method, which adopting the reciprocals of original variables as intervening variables in

2
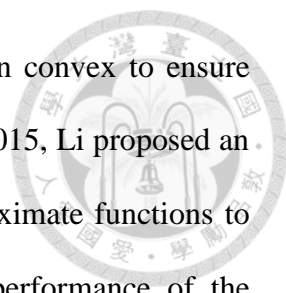
1st order Taylor series expansion [3]. This approximation method is quite suitable for stress and displacement constraint in simple truss problems when cross-section area is selected as design variable. However, the function value tends to infinity when the design variable approach zero that may cause inappropriate approximation. To overcome this problem, Haftka and Shore proposed modified reciprocal approximation method to shift the singular point in reciprocal approximation [4]. In 1979, Starnes and Haftka proposed conservative approximation method [5] which is also known as convex linearization (COLIN) presented by Fleury and Braibant [6]. This method adopts either direct linear or reciprocal approximation for each design variable, according to which approximate function is estimated higher. In other words, conservative approximation adopts the more conservative one between direct linear and reciprocal approximation for every design variable. In 1987, Svanberg presented the method of moving asymptotes (MMA), which can be regarded as the generalization of CONLIN [7].

To improve the approximation quality of single-point approximations, a lot of approximation schemes developed subsequently with utilizing the information of previous design point to construct approximate functions. These approximations are classified as two-point approximations. In 1987, Haftka et al. proposed two-point modified reciprocal approximation which has the strategy to decide the indeterminate coefficients in modified reciprocal approximation [8]. However, this strategy is undefined when the derivatives of two successive points have the different signs. In 1990, Fadel et al. proposed two-point exponential approximation (TPEA) [9]. TPEA performs Taylor series expansion with exponential intervening variables. The derivative of the previous design point is used to determine the exponent. But this approximation lacks definition for two-point approximation when the derivatives of the variable of two successive points have the different signs. In 1994 and 1995, Wang and Grandhi

3

proposed a series of two-point adaptive nonlinear approximations (TANA) based on TPEA, which enhance TPEA by matching the function value of previous design point [10][11]. In 1994, Snyman and Stander presented spherical approximation method (SAM) which appends a quadratic term to direct linear approximation for correcting the function value of the previous design point [12]. In 1995, Fadel classified the approximate functions into monotonic and non-monotonic functions [13]. It is suggested that the selection the approximations should consider the characteristic of monotonicity of the structural behavior. Then the mixed method is proposed named DQA-GMMA, which adopts monotonic approximation for design variable when the derivatives of two successive design points have the same signs, and vice versa.

In 1997, Zhang and Fleury proposed modified convex approximation (MCA) based on CONLIN [14]. MCA increases the convexity of approximation to avoid non-convergent process. In 1998, Xu and Grandhi proposed two-point adaptive nonlinear approximation-3 (TANA-3), which appends a term to TPEA for additionally matching the function value of previous design point [15]. In 2000, Xu et al. presented a new two-point approximation approach which uses the linear combination of linear and reciprocal approximations to match the derivatives of previous design point [16]. In 2001, Kim et al. presented two-point diagonal quadratic approximation (TDQA) based on TPEA [17]. TDQA adds shifting level into exponential intervening variables to avoid the singularity of the derivatives. In 1996, Chickermane and Gea proposed generalized convex approximation (GCA) [18]. GCA uses the derivatives of two points to construct approximate functions without lacking definition in TPEA. In 2007, Groenwold proposed incomplete series expansion (ISE) which includes a series of approximations [19]. ISE uses quadratic, cubic, and even higher order diagonal terms to construct the approximate functions.

4

Several approximation schemes have the approximate function convex to ensure stability of the optimization process such as GCMMA [20][21]. In 2015, Li proposed an adaptive quadratic approximation (AQA) which enforces the approximate functions to be strictly convex to improve the robustness and convergence performance of the optimization process [22]. However, this enforcement would cause inconsistency and may lower the efficiency of optimization process.

Moreover, Chiou proposed two new convex approximation methods in 2000, including self-adjusted convex approximation (SACA) and two-point convex approximation (TPCA) [23]. In 2002, Chen proposed improved two-point approximation (ITPA) which can be seen as the combination the linear-reciprocal and TPEA [24]. In 2007, Chang proposed quasi-quadratic two-point conservative approximation (QTCA) [25]. In 2010, Chen proposed exponential MMA (EMMA), which makes the order of intervening variables in MMA adjustable for more flexibility [26]. In 2012, Chen proposed a new mixed two-point approximation method which is the combination of TPEA and GBMMA [27]. In 2013, Jiang proposed enhanced two-point exponential approximation (ETPEA) to conquer the problem of lack of definition in TPEA [28]. ETPEA use intervening variable which is the second order Taylor series expansion of the original variable to deduce the new formula as the remedy of TPEA.

1.3   Strategies of research

The approximation quality is the crucial factor for the efficiency and stability in SAO process. This thesis presents a new approximation method, named two-point piecewise adaptive approximation (TPPAA). TPPAA is applied to construct the approximate functions of structural behavior such as stress, displacement and natural

5

frequency for optimization problems. The strategies are as follows:

(1) Review the existing approximation schemes and discuss the merits and defects of each method.

(2) Test some classical approximation methods in several optimization problems and compare the approximation quality in each case.

(3) Create the 1-D plot of the approximate functions in several cases to realize the characteristics of each approximation.

(4) The new method is developed and tested in several optimization problems to verify its practicability.
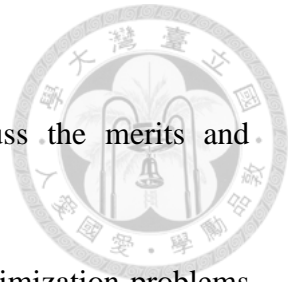
1.4   Outline

There are six chapter in this thesis:

Chapter 1: Introduce the development of structural optimization and the existing approximation methods briefly. After that, the research strategy of this study is mentioned.

Chapter 2: Introduce the procedure of mathematical optimization in this study and several existing approximation methods.

Chapter 3: Present the derivation of new approximation method developed in this study. Also the characteristics of the new method is compared with other approximation methods.

Chapter 4: Apply the proposed approximation method to several small scale structures and compare the results with other approximation methods.

Chapter 5: Apply the proposed approximation method to several large scale structures and compare the results with other approximation methods.

Chapter 6: Conclude the achievements and recommend the future work.

Chapter 2   Application of approximation methods in structural optimization
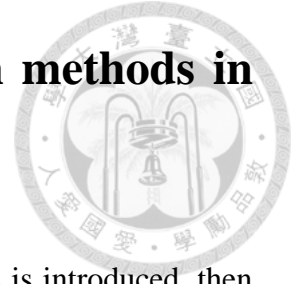
First, the procedure of mathematical optimization in this thesis is introduced, then several previous approximation methods are also discussed for the development of new approximation method.

2.1   Procedure of mathematical optimization

This section introduces the details of the mathematical optimization in sequence. The optimization problem can be written as

$$
\begin{aligned}
&\text{Find } \vec{x}, \\
&\text{such that } \quad F(\vec{x}) \rightarrow \min, \\
&\text{subject to } \quad g_i(\vec{x}) \leq 0, \quad i = 1, 2 \ldots, n_c,
\end{aligned}
\tag{2.1}
$$

where $\vec{x}$ denotes the design vector, $F(\vec{x})$ denotes the objective function to be minimized, $g_i(\vec{x})$ denotes the i-th constraint, n_c denotes the number of constraints.

2.1.1   Selection of design variables

The first step for optimization is defining the design variables for the problem. With taking efficiency in consideration, an optimization problem should prevent from having too many design variables. In order to reduce the design space, one of the solutions is to choose the dominant variables only instead of all the possible ones. Another way is to link the design variables, which can be expressed as

$$
\vec{x} = [T] \vec{X},
\tag{2.2}
$$

where $\vec{X}$ denotes the basis of original design vector, $\vec{x}$ is the reduced basis, and $[T]$ is the connectivity matrix of design variables.
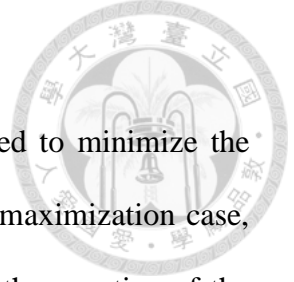
2.1.2 Defining objective function

In this study, the mathematical optimization problem is defined to minimize the objective function as the expression of Eq. (2.1). To deal with the maximization case, from another point of view, the problem is turned into minimizing the negative of the original objective function.

For the problem considering various objective functions, they are linked with appropriate weighted coefficients. It can be written as

$$F(\vec{x}) = \sum_{i=1} w_i F_i(\vec{x}), \tag{2.3}$$

where $F(\vec{x})$ denotes the total objective function, $F_i(\vec{x})$ denotes the individual objective function and w_i denotes the weighted coefficient.

2.1.3 Sensitivity analysis

Thanks to well-developed finite element method, the complicate structural analysis is available for optimization nowadays. Besides the response magnitude of structural behavior, the first order derivative, which also called sensitivity, is also required in the local approximation schemes and most search direction algorithms.

Sensitivity analysis is the way to realize the variation tendency of structural behavior with respect to design variables. In this study, backward difference method is adopted in sensitivity analysis, which can be expressed as

$$\frac{\partial h(\vec{x}_0)}{\partial x_i} = \frac{h(\vec{x}_0) - h(\vec{x}_0 - \Delta\vec{x}_i)}{\Delta x_i}, \tag{2.4}$$

where $\partial h(\vec{x}_0)/\partial x_i$ denotes the sensitivity of $h(\vec{x})$ with respect to x_i at $\vec{x}_0$, $\Delta\vec{x}_i = \{0\ 0\ 0\ ...\ \Delta x_i\ ...\ 0\}^T$ represents that only the i-th design variable has a small variation Δx_i.

8
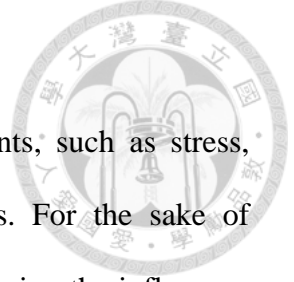
2.1.4 Treatment of constraints

In structural optimizations, there are many kinds of constraints, such as stress, displacement, natural frequency, size, and move limit constraints. For the sake of making the mathematical problem in the form as Eq. (2.1), and reducing the influences of numerical difference between different constraints, the constraints should be modified as follows.

A. Behavior constraint

To avoid the fracture of structures or large displacement which influences the performance of structures, stress and displacement constraints are often needed in structural optimizations. These two constraints can be expressed as

$$g_i^L \leq g_i \leq g_i^U, \quad i = 1, 2, ..., n_b,$$
$$g_i^L < 0, \quad g_i^U > 0,$$
(2.5)

where g_i^L and g_i^U denote the lower and upper bound of the i-th constraint respectively, and n_b denotes the number of behavior constraints. The constraints should be treated as

$$g_i^M = \begin{cases} \dfrac{g_i}{g_i^U} - 1.0, & \text{if } g_i \geq 0 \\[3mm] \dfrac{g_i}{g_i^L} - 1.0, & \text{if } g_i < 0 \end{cases} \quad i = 1, 2, ..., n_b,$$
(2.6)

where g_i^M denotes the modified constraints.

Moreover, to avoid resonance occurring, the natural frequencies of the structure are often restricted in certain region. The constraint of frequency can be expressed as

$$g_i^L \leq g_i, \quad i = 1, 2, ..., n_b,$$
$$g_i^L > 0.$$
(2.7)

The constraints should be treated as

9
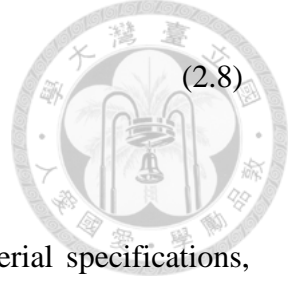
$$g_i^M = 1.0 - \frac{g_i}{g_i^L}, \quad i = 1, 2, ..., n_b.$$ (2.8)

B. Size constraint

Size constraints are the limits of design variables due to material specifications, practical demands, and so on. Size constraints can be expressed as

$$D_i^L \le x_i \le D_i^U, \quad i = 1, 2, ..., n_s,$$ (2.9)

where D_i^L and D_i^U denote the lower and upper bounds of allowable sizes respectively, and n_s denote the number of size constraints.

C. Move limit

In the local approximation, approximation is trustable only around the current design point. Hence move limit is introduced, which can be expressed as

$$\Delta x_i^L \le \Delta x_i \le \Delta x_i^U, \quad i = 1, 2, ..., n,$$ (2.10)

where Δx_i denotes the variation of the i-th design variable, Δx_i^L and Δx_i^U are lower and upper bound of the variations of the i-th design variable respectively and n denotes the number of design variables.

2.1.5 Application of approximation methods

Once the mathematical problem is defined, the optimal solution can be found by mathematical programming. However, the relation between structural behavior and design variables is implicit usually. Hence the approximation technique is applied to convert the implicit behavior into explicit functions. Because the approximated functions are constructed by current design point, the formed mathematical problem is not exactly the same as the real problem, but reliable near the current design point. So, to obtain the optimal solution, it requires to solve several optimization problems of approximated functions. Each sub-problem takes the optimal solution of last iteration as

10

the initial design. This gradual improvement process is known as sequential approximate optimization (SAO).
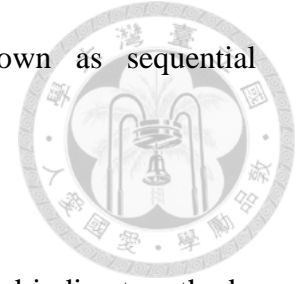
2.1.6 Application of mathematical optimization

Numerical optimization method can be classified into direct and indirect methods. Direct method such as method of feasible direction is to solve the optimization problems without transferring the constraints. Indirect method converts the constraints to a part of objective function, hence the constrained problems can be transferred to unconstrained problems.

Indirect method includes interior penalty method and exterior penalty method. When interior penalty method is adopted, the initial design must be in the feasible domain. However, it cannot guarantee that the initial design is always in the feasible domain in iterative process. So, exterior penalty method is adopted to deal with the constrained problems to make the process valid with infeasible initial design in this study. After transformation, the objective function can be expressed as

$$\Phi(\vec{x}, r) = F(\vec{x}) + r \sum_{j=1}^{n_c} < g_i(x) >^2,$$

$$< g_i(\vec{x}) > = \begin{cases} g_i(\vec{x}), & if \ g_i(\vec{x}) > 0 \\ 0, & if \ g_i(\vec{x}) \le 0 \end{cases},$$

(2.11)

where $\Phi(\vec{x}, r)$ denotes the penalized objective function, $F(\vec{x})$ is the objective function, r is the penalty factor and $g_i(x)$ denotes the i-th constraint function.

2.2 Single-point approximation methods

Single-point approximation methods use the function value and derivatives of single design point to construct the approximate function. Several existing single-point approximation methods are compared in this section.

11
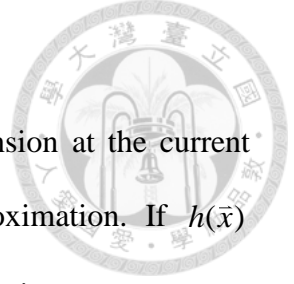
2.2.1 Direct linear approximation

This approximation method takes the first order Taylor expansion at the current design point. It is the most fundamental method of local approximation. If $h(\vec{x})$ denotes the function to be approximated, this approximation can be written as

$$h_l(\vec{x}) = h(\vec{x}_0) + \sum_{i=1}^{n} \frac{\partial h(\vec{x}_0)}{\partial x_i}(x_i - x_{0i}), \tag{2.12}$$

where $h_l(\vec{x})$ denotes the approximate function of direct linear approximation, $\vec{x}_0$ denotes the variable vector of current point with *i*-th component x_{0i}.

Since most behavior functions of general structures are nonlinear, this method may be not reliable.

2.2.2 Reciprocal approximation

The cross-section area of beams and the thickness of plates are often selected as the design variables, and the stress, displacement are often selected as constraints in structural optimization problems. In this kind of problem, the relation between the reciprocals of variables and the constraints are near linear for simple structures. Hence, in this case, performing 1st order Taylor series expansion in terms of reciprocals of the design variables would has the better approximation quality in comparison with direct linear approximation, which is called reciprocal approximation method [3].

$$h_r(\vec{x}) = h(\vec{x}_0) + \sum_{i=1}^{n} \frac{\partial h(\vec{x}_0)}{\partial x_i}(x_i - x_{0i})(\frac{x_{0i}}{x_i}), \tag{2.13}$$

where $h_r(\vec{x})$ denotes the approximate function of reciprocal approximation.

However, $x_i = 0$ is the singular point in this approximation method. When the design variable approaches to the singular point, the magnitude of the function value and derivative tend to infinity, and the approximation quality would be affected

therefore.

2.2.3 Modified reciprocal approximation

In order to conquer the defect of reciprocal approximation, Haftka proposed modified reciprocal approximation method [4]. The singular point is shifted to enlarge the reliable region. This approximation can be expressed as

$$h_{mr}(\vec{x}) = h(\vec{x}_0) + \sum_{i=1}^{n} \frac{\partial h(\vec{x}_0)}{\partial x_i}(x_i - x_{0i})(\frac{x_{0i} + x_{mi}}{x_i + x_{mi}}),$$ (2.14)

where $h_{mr}(\vec{x})$ denotes the approximate function of modified reciprocal approximation. The singular point is shifted from zero to $-x_{mi}$. But the determination of x_{mi} needs to depend on experience.

2.2.4 Conservative and convex approximation

Conservative approximation selects the more conservative one between direct linear and reciprocal approximations for each design variable [5][6]. So it can ensure that the function value would not less than neither direct linear nor reciprocal approximation. The idea of increasing the conservativeness is to make the solution of approximate problem satisfies the constraints more possible. The formula can be written as

$$h_c(\vec{x}) = h(\vec{x}_0) + \sum_{i=1}^{+} \frac{\partial h(\vec{x}_0)}{\partial x_i}(x_i - x_{0i}) + \sum_{i=1}^{-} \frac{\partial h(\vec{x}_0)}{\partial x_i}(x_i - x_{0i})\left(\frac{x_{0i}}{x_i}\right),$$ (2.15)

where $h_c(\vec{x})$ denotes the approximate function of convex approximation method,

$\sum_{i=1}^{+}$ denotes the summation of the design variable with positive first order derivative,

and $\sum_{i=1}^{-}$ denotes the summation of the design variable with negative first order derivative.

13

However, the too conservative approximation would reduce the convergence rate and result in low efficiency to the process.

2.3 Two-point approximation

Besides using the response value and sensitivity of current design, two-point approximation methods utilize the information of previous design point to improve approximation quality. Several existing two-point approximation methods are compared in this section.

2.3.1 Two-point modified reciprocal approximation

In 1987, Haftka proposed two-point modified reciprocal approximation method [8], which gives a recommendation on determining the indeterminate coefficient in modified reciprocal approximation method. So these two approximation methods have the same form.

$$h_{tmr}(\vec{x}) = h(\vec{x}_0) + \sum_{i=1}^{n} \frac{\partial h(\vec{x}_0)}{\partial x_i}(x_i - x_{0i})(\frac{x_{0i} + x_{mi}}{x_i + x_{mi}}), \quad (2.16)$$

where $h_{tmr}(\vec{x})$ denotes the approximate function of two-point modified reciprocal approximation and $\vec{x}_1$ denotes the variable vector of previous design point. x_{mi} is determined by matching the previous derivative and can be derived as

$$x_{mi} = \frac{x_{0i} - \eta_i x_{1i}}{\eta_i - 1}, \quad \eta_i = \sqrt{\frac{\partial h(\vec{x}_1)}{\partial x_i} \bigg/ \frac{\partial h(\vec{x}_0)}{\partial x_i}}. \quad (2.17)$$

Obviously, it is undefined when the two derivatives have the different signs. Moreover, x_{mi} is required to be a positive number to avoid the function value tending infinity, but it is not guaranteed in this method.

2.3.2 Two-point exponential approximation

In 1990, Fadel proposed two-point exponential approximation (TPEA) [9]. It takes

14

$x_i^{p_i}$ as the intervening variable for the first order Taylor series expansion.

$$h_{tpea}(\vec{x}) = h(\vec{x}_0) + \sum_{i=1}^{n} \frac{\partial h(\vec{x}_0)}{\partial x_i} \frac{x_{0i}^{1-p_i}}{p_i} \left(x_i^{p_i} - x_{0i}^{p_i} \right),$$ (2.18)

where $h_{tpea}(\vec{x})$ denotes the approximate function of TPEA. p_i is determined by fitting the derivative of the previous design point.

$$p_i = 1 + \frac{\ln\left[\dfrac{\partial h(\vec{x}_1)}{\partial x_i} \middle/ \dfrac{\partial h(\vec{x}_0)}{\partial x_i} \right]}{\ln\left(x_{1i}/x_{0i} \right)}.$$ (2.19)

However, this calculation lacks of definition under following two conditions:

$$\frac{\partial h(\vec{x}_1)}{\partial x_i} \middle/ \frac{\partial h(\vec{x}_0)}{\partial x_i} \le 0 \quad \text{or} \quad x_{1i}/x_{0i} \le 0.$$ (2.20)

When p_i cannot be calculated by matching the derivative, direct linear approximation is adopted instead. Besides that, p_i should be restricted in a specified range $p^L \le p_i \le p^U$ to avoid inappropriate approximation and $p^L = -1,\ p^U = 1$ is suggested by the author. When p_i is larger than p^U with calculated from Eq. (2.19), $p_i = p^U$ is adopted, and vice versa.

The approximate function of TPEA is always monotonic. However, non-monotonic approximation functions are required when the two derivatives of two successive design points have the different signs. Moreover, TPEA has the defect of singularity as reciprocal approximation when $p_i < 1$.

2.3.3 Linear-reciprocal approximation

In 2000, Xu presented linear-reciprocal approximation method [16]. With the linear combination of direct linear and reciprocal approximation methods, the derivative of the previous design point is matched.

15
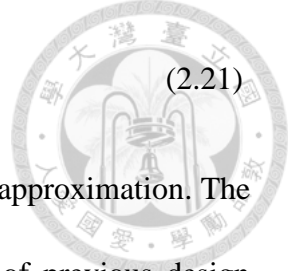
$$h_{lr}(\bar{x}) = h(\bar{x}_0) + \sum_{i=1}^{n} \alpha_i (x_i - x_{0i}) + \sum_{i=1}^{n} \beta_i (x_i - x_{0i}) \frac{x_{0i}}{x_i}, \quad (2.21)$$

where $h_{lr}(\bar{x})$ denotes the approximate function of linear-reciprocal approximation. The coefficients α_i and β_i are determined by matching the gradient of previous design point.

$$\beta_i = \frac{\dfrac{\partial h(\bar{x}_0)}{\partial x_i} - \dfrac{\partial h(\bar{x}_1)}{\partial x_i}}{1 - \left(\dfrac{x_{0i}}{x_{1i}}\right)^2}, \quad (2.22)$$

$$\alpha_i = \frac{\partial h(\bar{x}_0)}{\partial x_i} - \beta_i. \quad (2.23)$$

This method implies that with utilizing the linear combination of two different single-point approximations, a new two-point approximation method which matches the gradient of previous design point can be created arbitrarily.

2.3.4 Incomplete series expansion

In 2007, Groenwold proposed a series of approximations named incomplete series expansion (ISE) [19]. The fundamental idea of ISE is to approximate the Hessian matrix by excluding the off-diagonal terms for saving the computational requirements. The general form can be written as

$$h_{ise}(\bar{x}) = h(\bar{x}_0) + \sum_{i=1}^{n} \frac{\partial h(\bar{x}_0)}{\partial x_i} (x_i - x_{0i}) + \sum_{j=2}^{p} \sum_{i=1}^{n} c_{ji} |x_i - x_{0i}|^j, \quad (2.24)$$

where $h_{ise}(\bar{x})$ denotes the approximate function of ISE.

The simplest approximate form of ISE family is non-spherical quadratic ISE, which can be expressed as

$$h_{\nabla 2}(\bar{x}) = h(\bar{x}_0) + \sum_{i=1}^{n} \frac{\partial h(\bar{x}_0)}{\partial x_i} (x_i - x_{0i}) + \sum_{i=1}^{n} c_{2i} |x_i - x_{0i}|^2, \quad (2.25)$$

16

where $h_{\nabla 2}(\vec{x})$ denotes the approximate function of non-spherical quadratic ISE. This approximation method is the same as diagonal quadratic approximation (DQA) [13]. The coefficients are determined by matching the gradient of previous design point.

$$c_{2i} = \frac{\dfrac{\partial h(\vec{x}_1)}{\partial x_i} - \dfrac{\partial h(\vec{x}_0)}{\partial x_i}}{2(x_{1i} - x_{0i})}. \tag{2.26}$$

Another member of ISE named non-spherical cubic approximation which can additionally match the function value of previous point with $c_{2i} = c_2$, $i = 1, 2, ..., n$.

$$h_{nsc}(\vec{x}) = h(\vec{x}_0) + \sum_{i=1}^{n} \frac{\partial h(\vec{x}_0)}{\partial x_i}(x_i - x_{0i}) + c_2 \sum_{i=1}^{n} |x_i - x_{0i}|^2 + \sum_{i=1}^{n} c_{3i} |x_i - x_{0i}|^3, \tag{2.27}$$

where $h_{nsc}(\vec{x})$ denotes the approximate function of non-spherical cubic approximation.

In conclusion, ISE proposed a way to match extra information with arbitrary approximation forms. An approximate function can fit the derivative of another point by adding a non-spherical term and fit the extra function value by adding a spherical term. However, all the approximation functions of ISE are the non-monotonic form. Hence it is not appropriate to be applied to some structural behavior since their characteristics of monotonicity.

2.3.5 Two-point adaptive nonlinearity approximation-3

In 1998, Xu and Grandhi proposed two-point adaptive nonlinearity approximation-3 (TANA-3) [15], which appends a correction term to TPEA for matching the function value at previous design point.

$$h_{\text{tana3}}(\vec{x}) = h(\vec{x}_0) + \sum_{i=1}^{n} \frac{\partial h(\vec{x}_0)}{\partial x_i} \frac{x_{0i}^{1-p_i}}{p_i}(x_i^{p_i} - x_{0i}^{p_i}) + \frac{1}{2}\varepsilon(\vec{x}) \sum_{i=1}^{n} (x_i^{p_i} - x_{0i}^{p_i})^2, \tag{2.28}$$

where $h_{\text{tana3}}(\vec{x})$ denotes the approximate function of TANA-3. $\dfrac{1}{2}\varepsilon(\vec{x}) \sum_{i=1}^{n} (x_i^{p_i} - x_{0i}^{p_i})^2$ is

17

the appended correction term to TPEA, and $\varepsilon(\vec{x})$ can be expressed as

$$
\left\{
\begin{array}{l}
\varepsilon(\vec{x}) = \dfrac{K}{\sum\limits_{i=1}^{n}(x_i^{p_i} - x_{1i}^{p_i})^2 + \sum\limits_{i=1}^{n}(x_i^{p_i} - x_{0i}^{p_i})^2}, \\[4mm]
K = 2\left[h(\vec{x}_1) - h(\vec{x}_0) - \sum\limits_{i=1}^{n}\left(\dfrac{\partial h}{\partial x_i}\right)_{\vec{x}_0} \dfrac{x_{0i}^{1-p_i}}{p_i}(x_{1i}^{p_i} - x_{0i}^{p_i}) \right].
\end{array}
\right.
\tag{2.29}
$$

The characteristic of the appended term is that the first order derivative equals zero at x_{0i} and x_{1i}. So the determination of p_i is the same as in TPEA, and the same inappropriate approximation would encounter in TANA-3.

2.4   Integrated optimization program

In this study, the automated optimization program is developed in Microsoft Visual C++ 2015 with integrating AutoCAD 2002 and Ansys 15.0 APDL. The flow chart is shown in Fig. 2-1. The procedure is introduced briefly as follow:

(1) Define the optimization problem including design variables, initial design, objective function and constraints.

(2) Output "DesignVariable.lsp" for parametric modeling in AutoCAD 2002 if needed. The model is output as "model.sat".

(3) Output "DesignVariable.mac" for finite element analysis in Ansys 15.0 APDL. The results are output in .txt format.

(4) Read the analysis results from .txt files. Then, the approximate functions are constructed to form the sub-problem. The new design is obtained after the mathematical optimization.
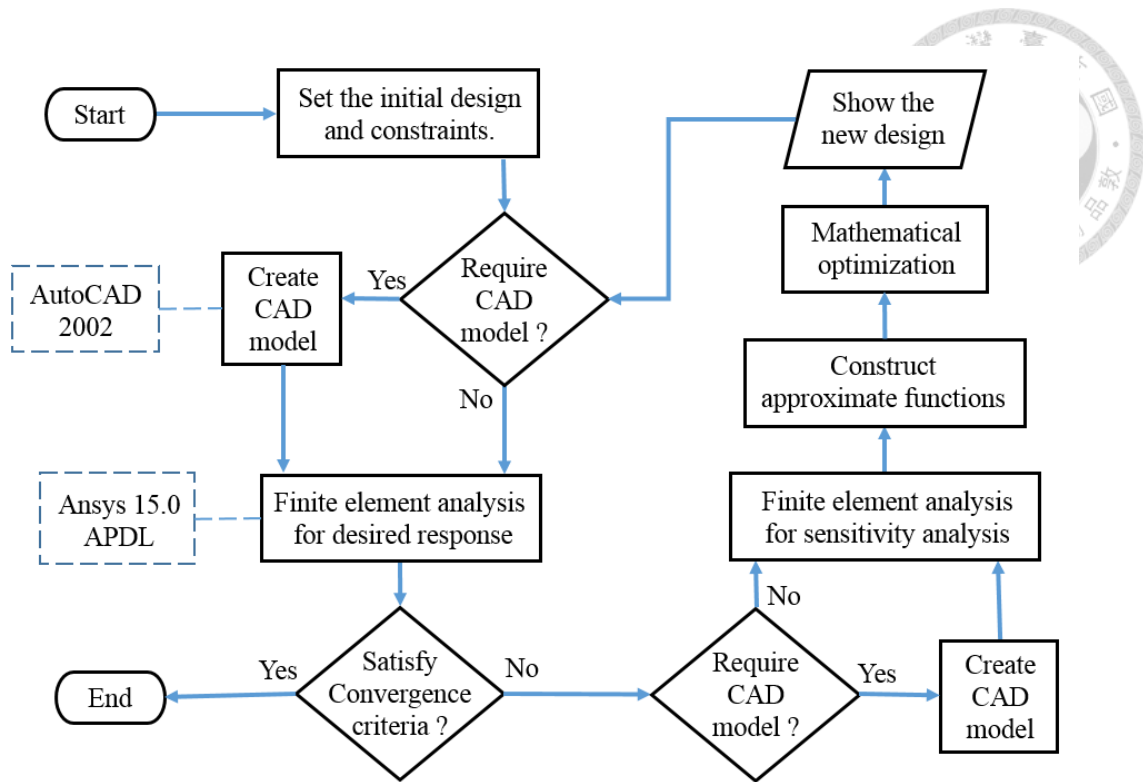
Fig. 2-1 Flow chart of developed optimization program

Chapter 3   The proposed approximation method

In this study, a new approximation method is proposed and named two-point piecewise adaptive approximation (TPPAA). Many kinds of structural behavior vary quasi-monotonically with respect to design variables. For this situation, monotonic functions are available in TPPAA when first order derivatives of two successive design points have the same signs. The non-monotonic form can be approximated also when the two first order derivatives have different signs. Moreover, the piecewise approximate functions are adopted to avoid the inappropriate approximation that the existing methods would encounter.

3.1   Modified incomplete series expansion

The fundamental idea of the proposed approximation method is to construct an approximate function of arbitrary order which matched the value of a point and first order derivatives of two points. In other words, it can construct approximate functions with arbitrarily specified nonlinearity degree, as shown in Fig. 3-1.
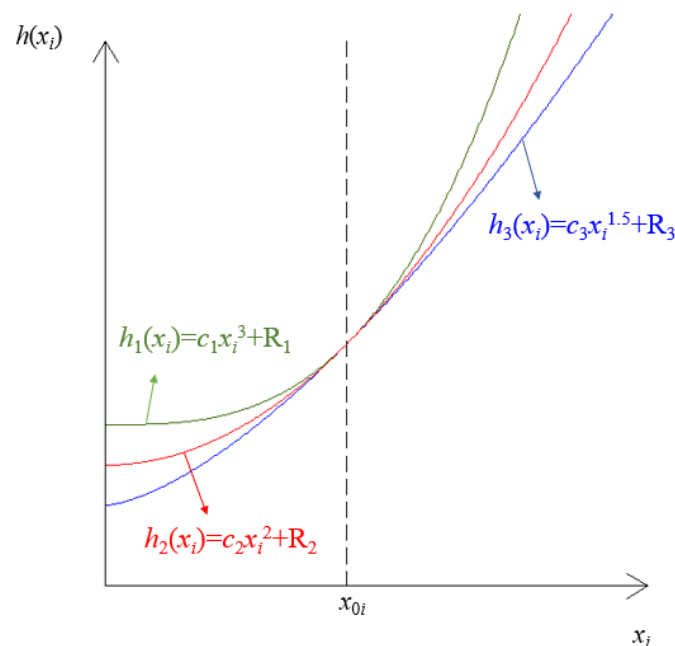
Fig. 3-1 Approximate functions with different orders

20
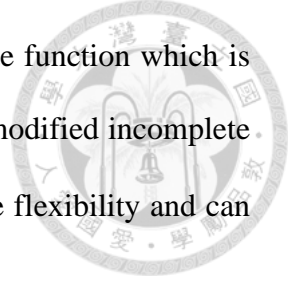
To avoid confusion, before introducing TPPAA, an approximate function which is based on ISE is discussed first. This new approximation, is named modified incomplete series expansion (MISE), also added the shifting term x_{mi} for more flexibility and can be expressed as

$$h_{mise}(\vec{x}) = h(\vec{x}_0) + \sum_{i=1}^{n} c_i |x_i - x_{mi}|^{p_i} - \sum_{i=1}^{n} R_i, \tag{3.1}$$

where $h_{mise}(\vec{x})$ denotes the approximate function of MISE, c_i, x_{mi}, p_i, R_i denote the coefficients to be determined. The differential form with respect to i-th variable is expressed as

$$\frac{\partial h_{mise}(\vec{x})}{\partial x_i} = p_i c_i \frac{|x_i - x_{mi}|^{p_i}}{x_i - x_{mi}}. \tag{3.2}$$

The essential requirement for local approximation is to fit the function value and derivatives at $\vec{x}_0$ and it can be achieved by determining c_i and R_i as follows with arbitrary p_i and x_{mi} given.

From Eq. (3.2), c_i can be determined by fitting the derivatives at $\vec{x}_0$.

$$c_i = \frac{\dfrac{\partial h(\vec{x}_0)}{\partial x_i}(x_{0i} - x_{mi})}{p_i |x_{0i} - x_{mi}|^{p_i}}. \tag{3.3}$$

Then, $\sum_{i=1}^{n} R_i$ is derived by fitting the function value at $\vec{x}_0$ and

$$R_i = c_i |x_{0i} - x_{mi}|^{p_i} \tag{3.4}$$

can be one of the solution. Hence R_i is expressed as

$$R_i = \frac{1}{p_i} \frac{\partial h(\vec{x}_0)}{\partial x_i}(x_{0i} - x_{mi}). \tag{3.5}$$

Because MISE is a kind of separable approximation (approximate function consists

21
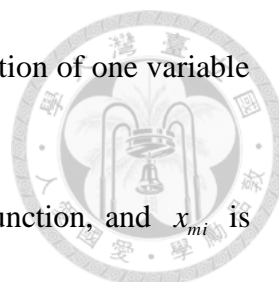
of several separable single-variable functions), the approximate function of one variable is discussed for simplicity in the following discussion.

When $p_i > 1$, the approximate function is a non-monotonic function, and x_{mi} is the extreme point, as shown in Fig. 3-2. Hence the sign of second order derivative is based on which side x_{mi} is with respect to x_{0i}. Fig. 3-2 shows the approximate functions of MISE which fit a point of $x_{0i} = 5$, $h(\bar{x}_0) = 3$, $\partial h(\bar{x}_0)/\partial x_i = -7$. $p_i = 2$, $x_{mi} = 3$ is given for $h_1(x_i)$ and $p_i = 2$, $x_{mi} = 7$ is given for $h_2(x_i)$.
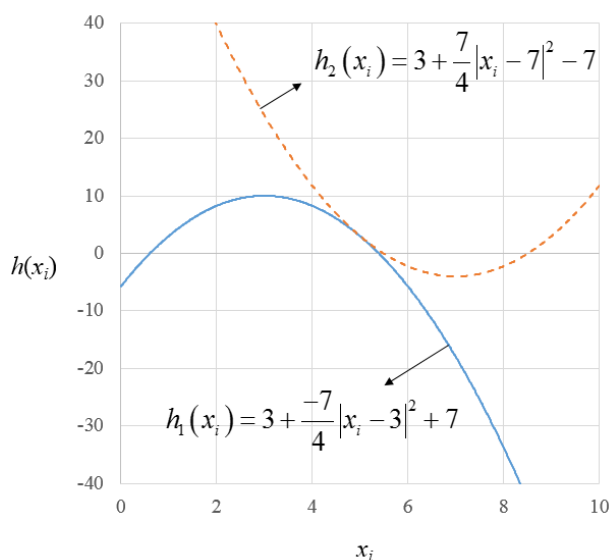
Fig. 3-2 Functions of MISE with $p_i > 1$

When $p_i < 1$, x_{mi} is the singular point, as shown in Fig. 3-3. The magnitude of derivative tends to infinity when the design variable x_i approaches to x_{mi}. Hence it may cause inappropriate approximation in general cases. Note that in the case of $p_i = -1$, $x_{mi} = 0$, MISE is the same as reciprocal approximation in $x_i > 0$, as shown in Eq. (2.13). Fig. 3-3 shows the approximate functions of MISE which fit a point of $x_{0i} = 5$, $h(\bar{x}_0) = 3$, $\partial h(\bar{x}_0)/\partial x_i = -7$. $p_i = 0.5$, $x_{mi} = 3$ is given for $h_1(x_i)$ and $p_i = 0.5$, $x_{mi} = 7$ is given for $h_2(x_i)$.

22
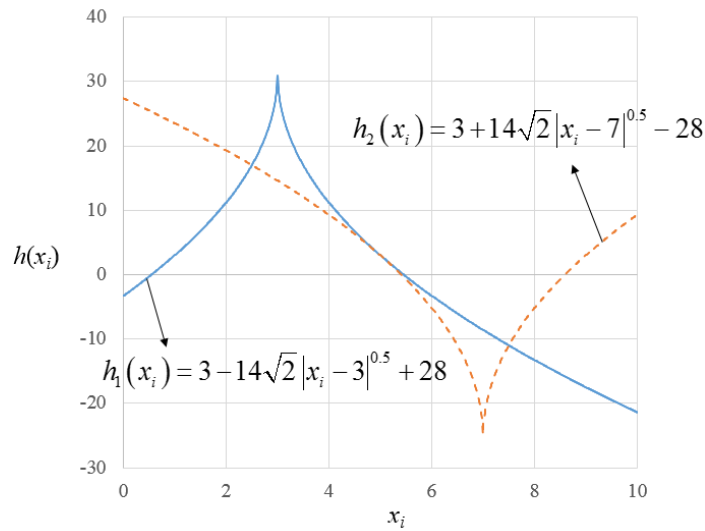
Fig. 3-3 Functions of MISE with $p_i < 1$

Though the information of current design point can be matched regardless of the selection of p_i and x_{mi}, the approximate function may vary a lot with different p_i and x_{mi} adopted as shown in Fig. 3-2 and Fig. 3-3. Hence the selection of p_i and x_{mi} is better to match the gradient at previous design point.

The gradient of previous point can be matched with either x_{mi} or p_i given, as explained in the following.

A.   Matching the gradient of previous point with given x_{mi}

To match the gradient of previous design point with x_{mi} given, p_i should be determined then. Substitute the derivative at $\bar{x}_1$ into the Eq. (3.2):

$$\frac{\partial h(\bar{x}_1)}{\partial x_i} = p_i c_i \frac{\left|x_{1i} - x_{mi}\right|^{p_i}}{x_{1i} - x_{mi}}. \tag{3.6}$$

With c_i derived in Eq. (3.3), Eq. (3.5) can be written as

$$\frac{\partial h(\bar{x}_1)}{\partial x_i} \Big/ \frac{\partial h(\bar{x}_0)}{\partial x_i} = \frac{\left(x_{0i} - x_{m_i}\right)}{\left(x_{1i} - x_{m_i}\right)} \times \frac{\left|x_{1i} - x_{m_i}\right|^{p_i}}{\left|x_{0i} - x_{m_i}\right|^{p_i}}. \tag{3.7}$$

23
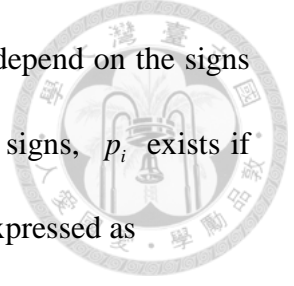
From Eq. (3.7), it is obvious that the selection of x_{mi} should depend on the signs

of the two derivatives. When the two derivatives have the different signs, p_i exists if

and only if x_{mi} is between x_{0i} and x_{1i}, and vice versa. It can be expressed as

$$\begin{cases} \left(x_{0i} - x_{m_i}\right)\left(x_{1i} - x_{m_i}\right) > 0, \text{ if } \dfrac{\partial h(\vec{x}_0)}{\partial x_i} \times \dfrac{\partial h(\vec{x}_1)}{\partial x_i} > 0 \\ \left(x_{0i} - x_{m_i}\right)\left(x_{1i} - x_{m_i}\right) < 0, \text{ if } \dfrac{\partial h(\vec{x}_0)}{\partial x_i} \times \dfrac{\partial h(\vec{x}_1)}{\partial x_i} < 0. \end{cases} \tag{3.8}$$

With the condition as Eq. (3.8) satisfied, Eq. (3.7) can be rewritten as

$$\left| \frac{\partial h(\vec{x}_1)}{\partial x_i} \middle/ \frac{\partial h(\vec{x}_0)}{\partial x_i} \right| = \frac{\left| x_{0i} - x_{m_i} \right|}{\left| x_{1i} - x_{m_i} \right|} \times \frac{\left| x_{1i} - x_{m_i} \right|^{p_i}}{\left| x_{0i} - x_{m_i} \right|^{p_i}} = \left| \frac{x_{1i} - x_{m_i}}{x_{0i} - x_{m_i}} \right|^{p_i - 1}. \tag{3.9}$$

Then p_i can be derived by taking the logarithm in Eq. (3.9).

$$p_i = 1 + \frac{\ln \left| \dfrac{\partial h(\vec{x}_1)}{\partial x_i} \middle/ \dfrac{\partial h(\vec{x}_0)}{\partial x_i} \right|}{\ln \left| \dfrac{x_{1i} - x_{mi}}{x_{0i} - x_{mi}} \right|}. \tag{3.10}$$

Note that when $\dfrac{\partial h(\vec{x}_0)}{\partial x_i}$ and $\dfrac{\partial h(\vec{x}_1)}{\partial x_i}$ have the same signs and $x_{mi} = 0$ is

adopted, MISE is the same as TPEA, as Eq. (2.18).

B. Matching the gradient of previous point with given p_i

To fit the gradient of previous design point with given p_i, x_{mi} should be

determined then. Under the premise of Eq. (3.8), Eq. (3.9) can be rewritten as

$$\begin{cases} \dfrac{\partial h(\vec{x}_1)}{\partial x_i} \middle/ \dfrac{\partial h(\vec{x}_0)}{\partial x_i} = \left(\dfrac{x_{1i} - x_{mi}}{x_{0i} - x_{mi}} \right)^{p_i - 1}, & \dfrac{\partial h(\vec{x}_1)}{\partial x_i} \times \dfrac{\partial h(\vec{x}_0)}{\partial x_i} > 0 \\ -\dfrac{\partial h(\vec{x}_1)}{\partial x_i} \middle/ \dfrac{\partial h(\vec{x}_0)}{\partial x_i} = \left(-\dfrac{x_{1i} - x_{mi}}{x_{0i} - x_{mi}} \right)^{p_i - 1}, & \dfrac{\partial h(\vec{x}_1)}{\partial x_i} \times \dfrac{\partial h(\vec{x}_0)}{\partial x_i} < 0. \end{cases} \tag{3.11}$$

Then x_{mi} can be derived as

24

$$
\begin{cases}
x_{mi} = x_{0i} - \dfrac{x_{1i} - x_{0i}}{\left(\dfrac{\partial h(\vec{x}_1)}{\partial x_i} \Big/ \dfrac{\partial h(\vec{x}_0)}{\partial x_i} \right)^{\frac{1}{p_i-1}} - 1}, & \dfrac{\partial h(\vec{x}_1)}{\partial x_i} \times \dfrac{\partial h(\vec{x}_0)}{\partial x_i} > 0 \\[3em]
x_{mi} = x_{0i} + \dfrac{x_{1i} - x_{0i}}{\left(-\dfrac{\partial h(\vec{x}_1)}{\partial x_i} \Big/ \dfrac{\partial h(\vec{x}_0)}{\partial x_i} \right)^{\frac{1}{p_i-1}} + 1}, & \dfrac{\partial h(\vec{x}_1)}{\partial x_i} \times \dfrac{\partial h(\vec{x}_0)}{\partial x_i} < 0.
\end{cases}
\tag{3.12}
$$

Note that when $p_i = 2$ is adopted, MISE is the same as DQA, as Eq. (2.25).

3.2 Two-point piecewise adaptive approximation

So far, with p_i given, the function value of current design and 1st derivatives of both design points can be matched in MISE. When the derivatives of two successive design points have the same signs, the approximate function is suggested to be monotonic. However, if $p_i > 1$ is adopted, the approximate function is always non-monotonic; if $p_i < 1$ is adopted, the approximate function exists singular point at x_{mi}, as shown in Fig. 3-4.
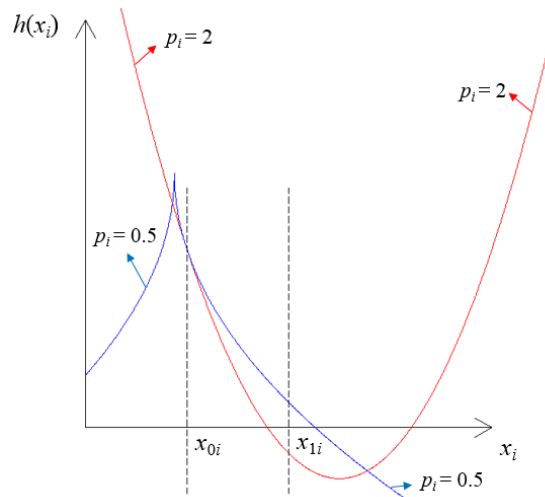
Fig. 3-4 Functions of MISE with different exponents

Hence the main idea of TPPAA is to use the piecewise function to overcome this dilemma. As illustrated in Fig. 3-4, $p_i > 1$ is adopted for averting the singular point in
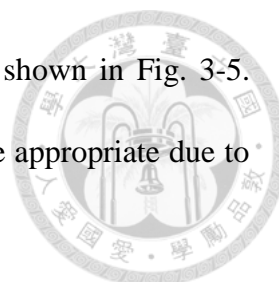
$x_i < x_{0i}$; $p_i < 1$ is adopted for the monotonic form in $x_i > x_{0i}$, as shown in Fig. 3-5. With the approximate function piecewise, the approximation is more appropriate due to the prevention of defects.
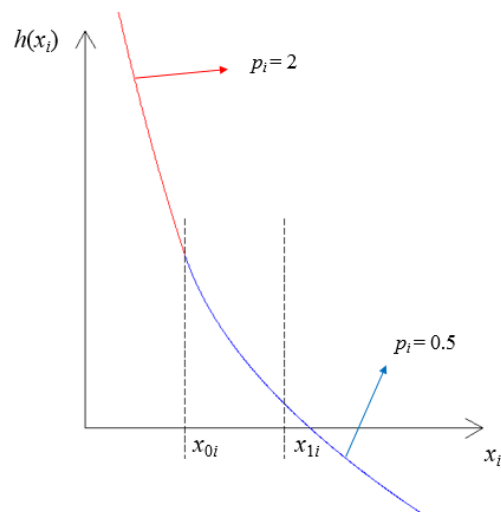
Fig. 3-5 Piecewise approximate function of TPPAA

Similarly, when the non-monotonic form is required, $p_i > 1$ is adopted to avoid singularity. Since the approximate function is piecewise when the monotonic form is required, the calculation of coefficients in MISE should depend on x_i. Hence, TPPAA is expressed as

$$h_{tppaa}(\vec{x}) = h(\vec{x}_0) + \sum_{i=1}^{n} c_i(x_i)|x_i - x_{mi}(x_i)|^{p_i(x_i)} - \sum_{i=1}^{n} R_i(x_i),\tag{3.13}$$

where $h_{tpaea}(\vec{x})$ denotes the approximate function of TPPAA. As just mentioned, $p_i(x_i)$ is assigned first in TPPAA, which is expressed as

$$\begin{cases} \text{if} \quad \dfrac{\partial h(\vec{x}_0)}{\partial x_i} \times \dfrac{\partial h(\vec{x}_1)}{\partial x_i} > 0, \\ \qquad \begin{cases} \text{if } (x_i - x_{0i}) \times (x_{pi} - x_{qi}) < 0, \ p_i(x_i) = p_{1i} > 1, \\ \text{if } (x_i - x_{0i}) \times (x_{pi} - x_{qi}) > 0, \ p_i(x_i) = p_{2i} < 1, \end{cases} \\ \text{else} \qquad p_i(x_i) = p_{3i} > 1, \end{cases}\tag{3.14}$$

26

where x_{pi} and x_{qi} are determined as

$$x_{pi} = \begin{cases} x_{0i}, & \text{for } \left|\dfrac{\partial h(\vec{x}_0)}{\partial x_i}\right| < \left|\dfrac{\partial h(\vec{x}_1)}{\partial x_i}\right| \\ x_{1i}, & \text{for } \left|\dfrac{\partial h(\vec{x}_1)}{\partial x_i}\right| < \left|\dfrac{\partial h(\vec{x}_0)}{\partial x_i}\right|, \end{cases} \qquad x_{qi} = \begin{cases} x_{0i}, & \text{for } \left|\dfrac{\partial h(\vec{x}_0)}{\partial x_i}\right| > \left|\dfrac{\partial h(\vec{x}_1)}{\partial x_i}\right| \\ x_{1i}, & \text{for } \left|\dfrac{\partial h(\vec{x}_1)}{\partial x_i}\right| > \left|\dfrac{\partial h(\vec{x}_0)}{\partial x_i}\right|. \end{cases} \tag{3.15}$$

p_{1i} denotes the given exponent which is greater than 1 when the monotonic form is required. p_{2i} denotes the given exponent which is less than 1 when the monotonic form is required. p_{3i} denotes the given exponent when the non-monotonic form is required. In this study, $p_{1i} = 2$, $p_{2i} = -2$ and $p_{3i} = 2$ is adopted.

Afterward, $c_i(x_i)$, $R_i(x_i)$, $x_{mi}(x_i)$ are derived as the same way in MISE.

$$c_i(x_i) = \frac{\dfrac{\partial h(\vec{x}_0)}{\partial x_i}(x_{0i} - x_{mi}(x_i))}{p_i(x_i)|x_{0i} - x_{mi}(x_i)|^{p_i(x_i)}}. \tag{3.16}$$

$$R_i(x_i) = \frac{1}{p_i(x_i)}\frac{\partial h(\vec{x}_0)}{\partial x_i}(x_{0i} - x_{mi}(x_i)). \tag{3.17}$$

$$\begin{cases} x_{mi}(x_i) = x_{0i} - \dfrac{x_{1i} - x_{0i}}{\left(\dfrac{\partial h(\vec{x}_1)}{\partial x_i} \Big/ \dfrac{\partial h(\vec{x}_0)}{\partial x_i}\right)^{\frac{1}{p_i(x_i)-1}} - 1}, & \dfrac{\partial h(\vec{x}_1)}{\partial x_i} \times \dfrac{\partial h(\vec{x}_0)}{\partial x_i} > 0 \\[4em] x_{mi}(x_i) = x_{0i} + \dfrac{x_{1i} - x_{0i}}{\left(-\dfrac{\partial h(\vec{x}_1)}{\partial x_i} \Big/ \dfrac{\partial h(\vec{x}_0)}{\partial x_i}\right)^{\frac{1}{p_i(x_i)-1}} + 1}, & \dfrac{\partial h(\vec{x}_1)}{\partial x_i} \times \dfrac{\partial h(\vec{x}_0)}{\partial x_i} < 0. \end{cases} \tag{3.18}$$

One of the merit of TPPAA is that design variables are not required to be non-negative. Moreover, TPPAA is sensitive to neither translation nor scaling of the design variables. The comparison between TPPAA and other existing approximation methods are listed in Table 3-1.

27

Table 3-1 Comparison of two-point approximation methods

Approximation method	Match previous design point		Approximate monotonic function	Approximate non-monotonic function	Existing singular point
	Function value	Gradient			
TPPAA	no	yes	yes	yes	no
TPEA	no	yes	yes	no	yes
Two-point modified reciprocal	no	yes	yes	no	yes
Linear-reciprocal	no	yes	no	no	yes
DQA	no	yes	no	yes	no
TANA-3	yes	yes	no	no	yes

3.3   Modification for convex approximation

To make optimization process more stable, several existing approximation methods enforce the approximate function of the i-th design variable to be convex or even strictly convex when

$$\left(x_{0i} - x_{1i}\right)\left(\frac{\partial h\left(\vec{x}_0\right)}{\partial x_i} - \frac{\partial h\left(\vec{x}_1\right)}{\partial x_i}\right) < 0. \tag{3.19}$$

However, this enforcement may cause inconsistency and affect the efficiency of process. Hence in this study, the approximate function of the i-th design variable in TPPAA is modified to be strictly convex only when

$$\left|x_{0i} - x_{1i}\right| < \delta \tag{3.20}$$

where δ is a given positive number.

The expression of the TPPAA with the modification adopted in this study can be written as

28

$$\tilde{h}_{tppaa}(\vec{x}) = h(\vec{x}_0) + \sum_{i=1}^{n} A_i \left\{ c_i(x_i) \left| x_i - x_{mi}(x_i) \right|^{p_i(x_i)} - \sum_{i=1}^{n} R_i(x_i) \right\}$$
$$+ \sum_{i=1}^{n} B_i \left\{ \frac{\partial h(\vec{x}_0)}{\partial x_i}(x_i - x_{0i}) + \varepsilon(x_i - x_{0i})^2 \right\}, \tag{3.21}$$

where A_i and B_i are determined as

$$\begin{cases} A_i = 0, \ B_i = 1, \ \ \text{for} \left| x_{0i} - x_{1i} \right| \le \delta \\ A_i = 1, \ B_i = 0, \ \ \text{for} \left| x_{0i} - x_{1i} \right| > \delta \end{cases} \tag{3.22}$$

and ε is a given positive number.

3.4 Modification for matching function value of previous design point

Several approximation methods do not match the function value of the previous design point, including TPPAA. A strategy for correcting this bias may be considered, that uses the linear combination with arbitrary two approximation methods which both match the function value at current design point and gradients of the two successive design points. This strategy is similar with linear-reciprocal approximation, which can be expressed as

$$h_{new}(\vec{x}) = \alpha h_{approx1}(\vec{x}) + (1-\alpha) h_{approx2}(\vec{x}),$$
$$\alpha = \frac{h(\vec{x}_1) - h_{approx2}(\vec{x}_1)}{h_{approx1}(\vec{x}_1) - h_{approx2}(\vec{x}_1)}, \tag{3.23}$$

where $h_{new}(\vec{x})$ denotes the new approximate function which matches the function value at previous design point with the linear combination of the two approximate functions $h_{approx1}(\vec{x})$ and $h_{approx2}(\vec{x})$.

However, with the strategies which match the function value at previous design point applied, it may cause the approximate function multimodal with respect to a

29
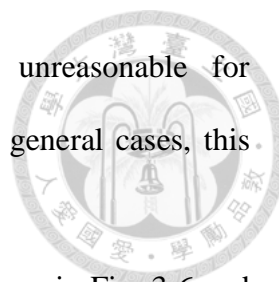
design variable. Since this kind of approximate function is unreasonable for representing structural behavior with respect to design variables in general cases, this strategy is not adopted in this study.

The examples of the multimodal approximate functions are shown in Fig. 3-6 and Fig. 3-7 with $x_{0i} = 2$, $h(\vec{x}_0) = 3$, $\partial h(\vec{x}_0)/\partial x_i = -3$, $x_{1i} = 4$, $h(\vec{x}_1) = 2$, $\partial h(\vec{x}_1)/\partial x_i = -1$. Fig. 3-6 shows the linear-reciprocal approximation with the correction term of TANA-3 appended. Fig. 3-7 shows the linear combination of TPPAA and DQA.
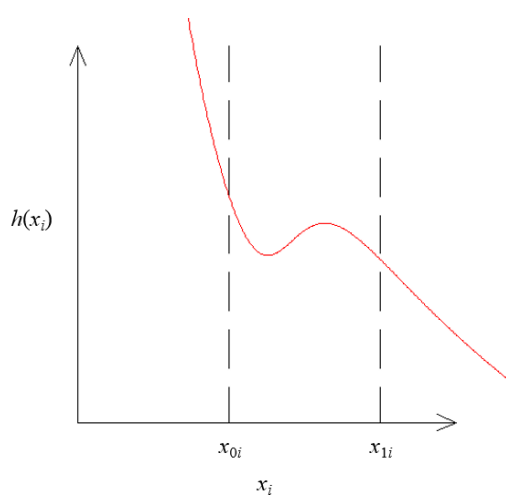
Fig. 3-6 Illustration of linear-reciprocal approximation with correction term of TANA-3

appended
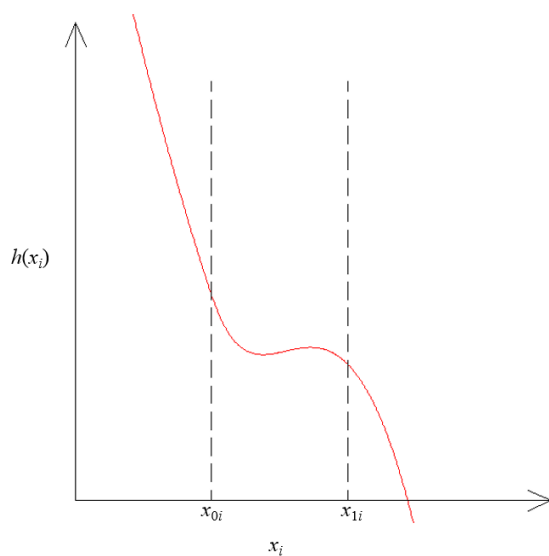
Fig. 3-7 Illustration of linear combination of TPPAA and DQA

30

Chapter 4   Optimization of small scale structures

The performance of TPPAA is examined by several structural optimization problems in this chapter. The comparison with previous approximation methods is also presented. The convergence criterion adopted in this chapter is that the relative difference of two consecutive objective function values is smaller than 0.1%. The specifications of computer used for the examples in this chapter is Intel i7-920 2.67GHz CPU with 4GB DDR3-1333 RAM.

4.1   2-bar truss

The 2-bar truss structure with a concentrated force acting on its top is shown in Fig. 4-1. The design data is listed in Table 4-1. The first design variable is the cross-section area of both bars and the second one is the supporting locations. The goal of the optimization is to minimize the total weight. This optimization problem considers sizing design and shape design simultaneously. The analytical expression can be derived as

$$\text{minimize } F\left(\bar{x}\right) = x_1\sqrt{1+x_2^2},$$

$$\text{subject to } \begin{cases} \sigma_1 = 0.124\sqrt{1+x_2^2}\left(\dfrac{8}{x_1}+\dfrac{1}{x_1 x_2}\right) \leq 1 \\[4mm] \sigma_2 = 0.124\sqrt{1+x_2^2}\left(\dfrac{8}{x_1}-\dfrac{1}{x_1 x_2}\right) \leq 1. \end{cases} \tag{4.1}$$

31
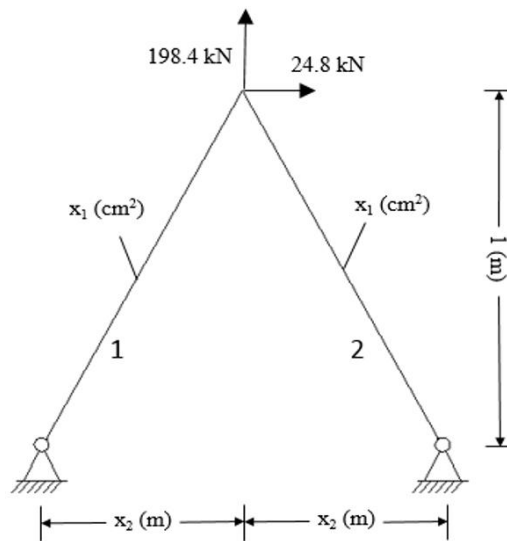
Fig. 4-1 2-bar truss structure

Table 4-1 Design data for 2-bar truss optimization

Constraints	Stress	$\sigma_i \leq 100 \dfrac{N}{mm^2}$ for each bar
	Size	0.2 cm$^2 \leq x_1 \leq 4.0$ cm^2 0.1 m $\leq x_2 \leq 1.6$ m
	Move limit	$0.75x_i^{(k-1)} \leq x_i^{(k)} \leq 1.25x_i^{(k-1)}$, $i = 1, 2$
Initial design		$x_1 = 1.5$ cm^2, $x_2 = 0.5$ m

Conservative approximation is adopted to construct the single-point approximate functions for the initial design. The SAO result of TPPAA is shown in Table 4-2 and Fig. 4-2, and the comparison with previous approximation methods is shown in Table 4-3. The CPU time of optimization process is 16 seconds. The exact solution of design variables is $(x_1, x_2) = (1.412, 0.377)$ and the objective function is 1.50865 (kgf).

32

Table 4-2 Result of TPPAA in 2-bar optimization

	x_1	x_2	Weight (kgf)
Initial design	1.500	0.500	1.6771
Iteration 1	1.386	0.375	1.4707
Iteration 2	1.413	0.375	1.5088
Optimum design	1.410	0.381	1.5086
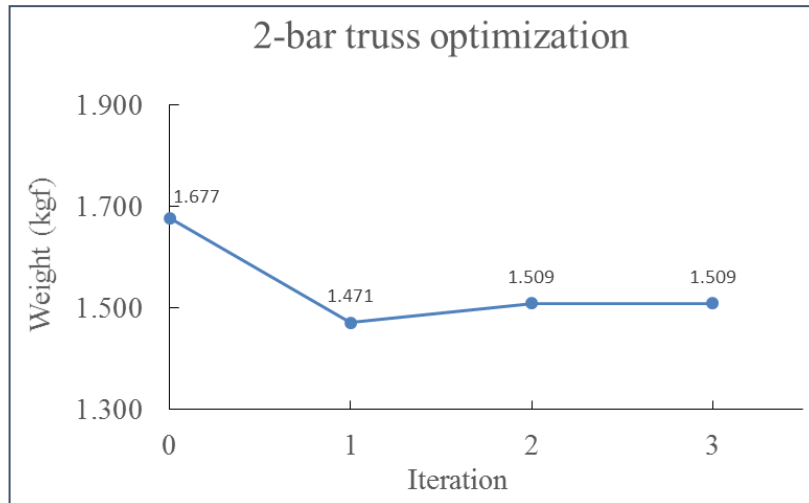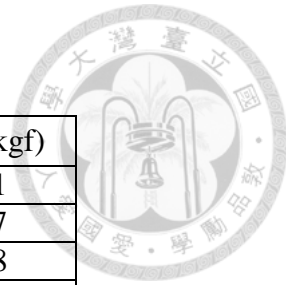
Fig. 4-2 Iteration history of weight of 2-bar truss

Table 4-3 Result comparison for 2-bar truss optimization

Approximation method	Iterations	Weight (kgf)
TPPAA	3	1.5086
DQA	3	1.5087
TPEA	3	1.5086
Direct linear	3	1.5087
Linear-reciprocal	3	1.5086

4.2   3-bar truss optimization

The 3-bar truss structure with a concentrated force acting on it is shown in Fig. 4-3. The design data are listed in Table 4-4. One of the design variables (x_1) represents the cross-section areas of bar 1 and bar 3, and the other one (x_2) represents the cross-section area of bar 2. The total weight of the 3-bar structure is the objective

33

function to be minimized. In this simple case, the stress constraints can be expressed in analytical form, thus the exact solution can be obtained for comparison. The exact solution of design variables is $(x_1, x_2) = (0.7887, 0.4082)$ and that of objective function is 26.3896 (lb).

Fig. 4-3 3-bar truss structure

Table 4-4 Design data for 3-bar truss optimization

Material property		$E = 30000\ ksi,\ \rho = 0.1\ lb/in^3,\ \nu = 0.3$
Constraints	Stress	$-15\ ksi \le \sigma_i \le 20\ ksi$ for each bar
	Size	$0\ in^2 \le x_i,\ i = 1, 2$
	Move limit	$\dfrac{x_i^{(k-1)}}{3} \le x_i^{(k)} \le 3x_i^{(k-1)},\ i = 1, 2$
Initial design		$x_1 = 2.0\ in^2,\ x_2 = 1.0\ in^2$

Conservative approximation is adopted to construct the single-point approximate functions for the initial design. The CPU time for the optimization process is 12 seconds. The SAO result of TPPAA is shown in Table 4-5 and Fig. 4-4. The comparison with existing approximation methods is shown in Table 4-6.

34

Table 4-5 Result of TPPAA in 3-bar truss optimization

	x_1	x_2	Weight (lb)
Initial design	2.000	1.000	66.569
Iteration 1	0.792	0.400	26.392
Optimum design	0.790	0.403	26.390
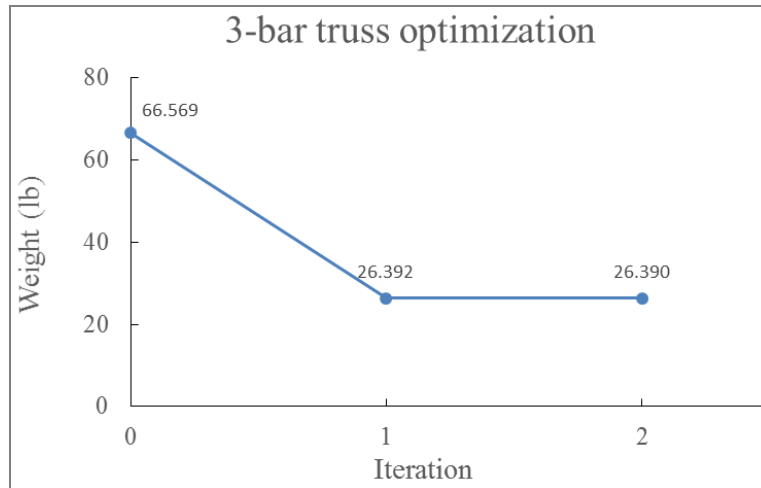
Fig. 4-4 Iteration history of weight of 3-bar truss

Table 4-6 Result comparison for 3-bar truss optimization

Approximation method	Iterations	Weight (lb)
TPPAA	2	26.390
DQA	2	26.390
TPEA	2	26.390
Linear-reciprocal	2	26.390
CONLIN	2	26.390

4.3   4-bar truss optimization

The 4-bar truss structure with a concentrated force acting on its top is shown in Fig. 4-5, and the design data is listed in Table 4-7. The objective function is the total weight of the 4-bar structure with the cross-section area of each bar selected as design variable.
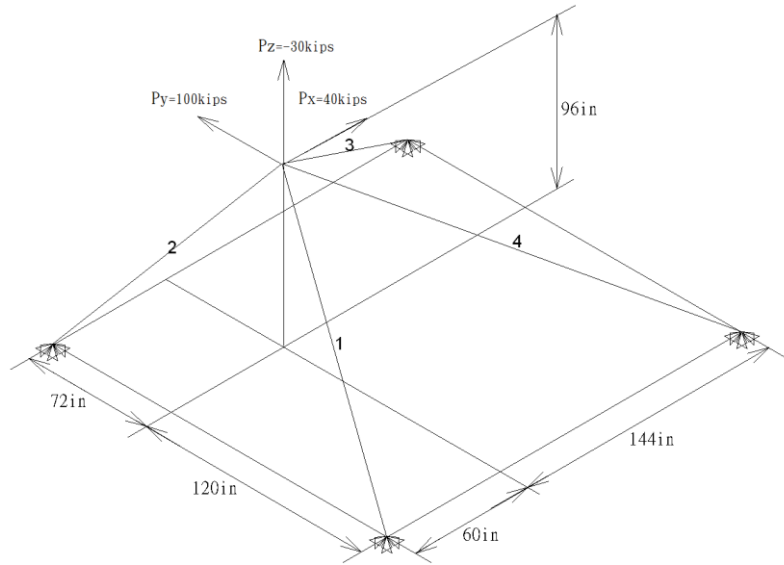
Fig. 4-5 4-bar truss structure

Table 4-7 Design data for 4-bar truss optimization

Material property		$E = 10000\ ksi,\ \rho = 0.1\ lb/in^3,\ \nu = 0.29$
Constraints	Stress	$-25\ ksi \leq \sigma_i \leq 25\ ksi$ for each bar
	Size	$1.0 \times 10^{-4}\ in^2 \leq x_i,\ i = 1, 2, 3, 4$
	Move limit	$\dfrac{x_i^{(k-1)}}{6.5} \leq x_i^{(k)} \leq 6.5 x_i^{(k-1)},\ i = 1, 2, 3, 4$
Initial design		$x_i = 2.0\ in^2,\ i = 1, 2, 3, 4$

Direct linear approximation is adopted to construct the single-point approximate functions for the initial design. The CPU time for the optimization process is 39 seconds. Result of SAO with TPPAA is shown in Table 4-8 and Fig. 4-6 respectively. Moreover, the comparison with previous approximation methods is shown in Table 4-9.

36

Table 4-8 Result of 4-bar truss optimization

	x_1	x_2	x_3	x_4	Weight (lb)
Initial design	2.000	2.000	2.000	2.000	139.44
Iteration 1	2.451	2.190	2.243	0.308	118.35
Iteration 2	2.667	2.300	2.159	0.047	116.32
Iteration 3	2.662	2.296	2.161	0.007	115.39
Iteration 4	2.663	2.298	2.160	0.001	115.27
Optimum design	2.663	2.298	2.159	0.0002	115.25
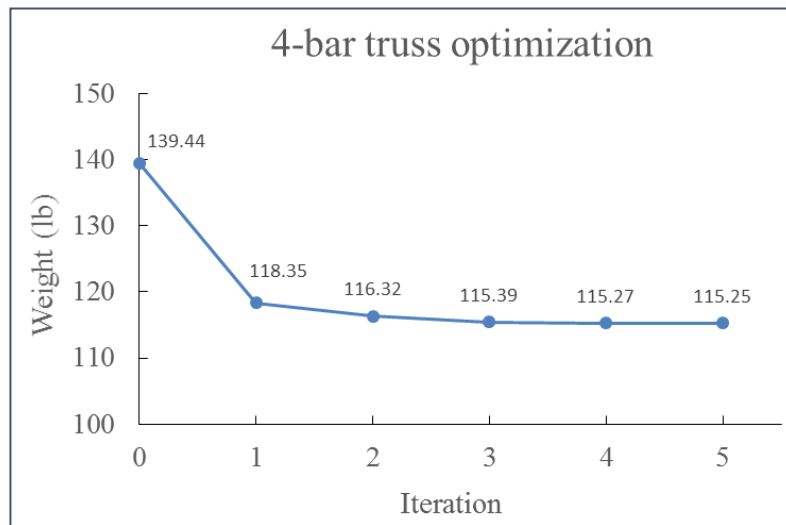
Fig. 4-6 Iteration history of weight of 4-bar truss

Table 4-9 Result comparison for 4-bar truss optimization

Approximation method	Iterations	Weight (lb)
TPPAA	5	115.25
DQA	5	115.25
TPEA	4	115.27*
Direct linear	5	115.25
TPEA-GBMMA [27]	4	115.28*
ETPEA1 [28]	4	115.28*

(*: premature convergence)

4.4　6-bar truss optimization

The 6-bar truss structure with a concentrated force acting on its end is shown in Fig. 4-7. The design data is listed in Table 4-10. The objective function is the total weight of the 6-bar structure with the cross-section area of each bar selected as design variable.
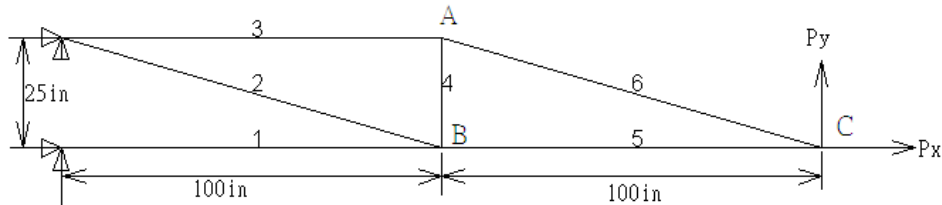
Fig. 4-7 6-bar truss structure

Table 4-10 Design data for 6-bar truss optimization

Material property		$E = 10000\ ksi,\ \rho = 0.1\ lb/in^3,\ \nu = 0.29$
Constraints	Displacement	$u_x \leq 20\ in,\ u_y \leq 40\ in$ for node A,B,C
	Size	$0.5\ in^2 \leq x_i \leq 10\ in^2,\ i = 1,2,...,6$
	Move limit	$\dfrac{x_i^{(k-1)}}{5} \leq x_i^{(k)} \leq 5x_i^{(k-1)},\ i = 1,2,...,6$
Initial design		$x_i = 2.0\ in^2,\ i = 1,2,...,6$

The CPU time for the optimization process is 39 seconds. Conservative approximation is adopted to construct the single-point approximate functions for the initial design. The SAO result of TPPAA is shown in Table 4-11 and Fig. 4-8 respectively, and the comparison with previous approximation methods is shown in Table 4-12.

38

Table 4-11 Result of TPPAA in 6-bar truss optimization

|	x_1	x_2	x_3	x_4	x_5	x_6	Weight (lb)
Initial design	2.000	2.000	2.000	2.000	2.000	2.000	106.23
Iteration 1	2.717	1.320	1.281	0.500	1.432	1.320	82.770
Optimum design	2.717	1.320	1.281	0.500	1.432	1.320	82.770
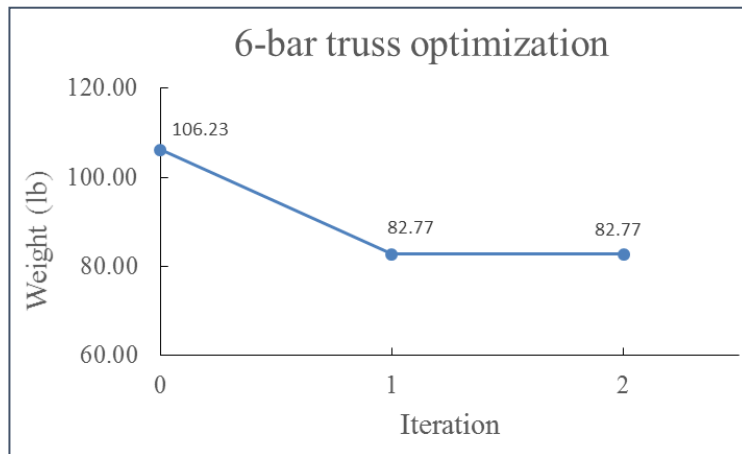
Fig. 4-8 Iteration history of weight of 6-bar truss

Table 4-12 Result comparison for 6-bar truss optimization

Approximation method	Iterations	Weight (lb)
TPPAA	2	82.770
DQA	2	82.770
TPEA	2	82.770
Direct linear	2	82.770

4.5   10-bar truss optimization

The weight minimization problem of 10-bar truss structure with a concentrated force acting on its end is shown in Fig. 4-9 (a=360 in). The design data is listed in Table 4-13. The objective function is the total weight of the 10-bar structure with the cross-section area of each bar selected as design variable.
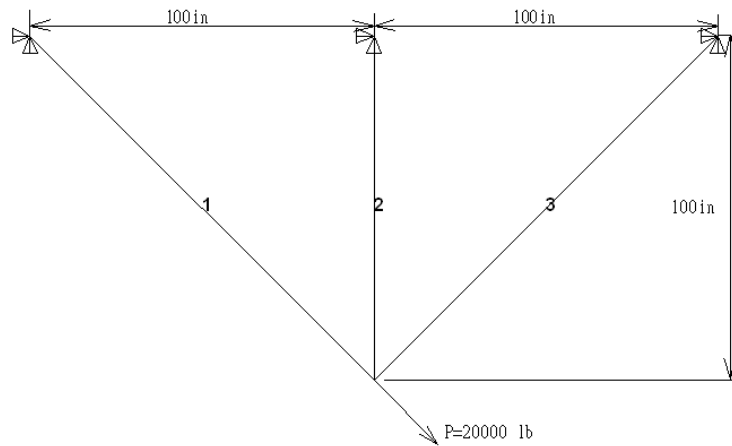
39
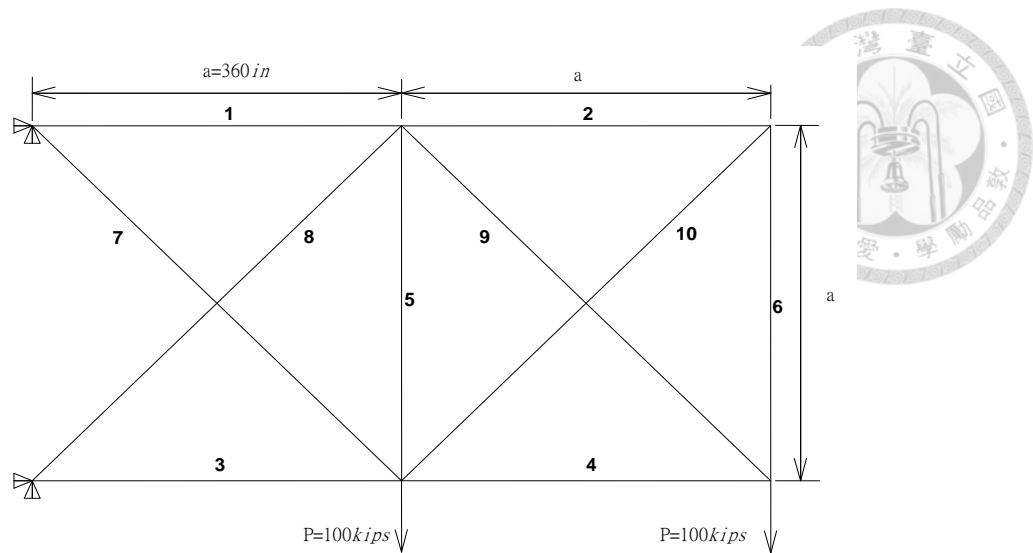
Fig. 4-9 10-bar truss structure

Table 4-13 Design data for 10-bar truss optimization

Material property		$E = 10000\ ksi,\ \rho = 0.1\ lb/in^3,\ \nu = 0.29$
Constraints	Stress	$-25\ ksi \le \sigma_i \le 25\ ksi,\ i = 1,2,...,8\ and\ 10$ $-75\ ksi \le \sigma_i \le 75\ ksi,\ i = 9$
	Size	$0.1\ in^2 \le x_i,\ i = 1,2,...,10$
	Move limit	$\dfrac{x_i^{(k-1)}}{3} \le x_i^{(k)} \le 3x_i^{(k-1)},\ i = 1,2,...,10$
Initial design		$x_i = 5.0\ in^2,\ i = 1,2,...,10$

The CPU time for the optimization process is 96 seconds. Conservative approximation is adopted to construct the single-point approximate functions for the initial design. The SAO result of TPPAA is shown in Table 4-14 and Fig. 4-10. The comparison with previous approximation methods is shown in Table 4-15. TPAEA with large δ is also tested in this example. δ is selected to be large enough so that the convex substitute functions are always adopted for approximation. The result shows that with too large δ adopted, the SAO process is stable but inefficient.

40

Table 4-14 Result of TPPAA in 10-bar truss optimization

|	x_1	x_2	x_3	x_4	x_5	x_6	x_7	x_8	x_9	x_{10}	Weight (lb)
Initial design	5.000	5.000	5.000	5.000	5.000	5.000	5.000	5.000	5.000	5.000	2098.2
Iteration 1	8.404	1.667	8.393	2.882	3.139	1.667	6.458	7.557	2.590	2.294	1903.6
Iteration 2	7.556	0.556	8.578	3.558	1.046	0.556	6.420	6.275	2.898	0.899	1626.2
Iteration 3	7.687	0.234	8.335	3.766	0.349	0.234	6.187	5.117	3.431	0.300	1507.3
Iteration 4	7.930	0.100	8.076	3.900	0.116	0.100	5.780	5.592	3.664	0.147	1501.0
Iteration 5	7.899	0.100	8.101	3.900	0.100	0.100	5.800	5.513	3.677	0.141	1497.6
Optimum design	7.900	0.100	8.100	3.900	0.100	0.100	5.798	5.515	3.677	0.141	1497.6
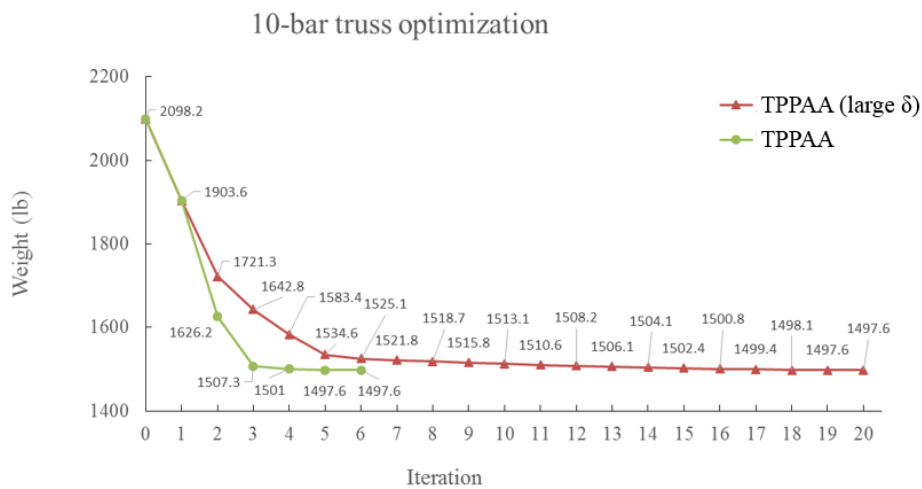
Fig. 4-10 Iteration history of weight of 10-bar truss

Table 4-15 Result comparison for 10-bar truss optimization

Approximation method	Iterations	Weight (lb)
TPPAA	6	1497.6
TPPAA (large δ)	20	1497.6
DQA	6	1497.6
Direct linear	7	1497.6
TPEA-GBMMA [27]	6	1497.6
ETPEA1 [28]	6	1497.6

(*: different convergence criterion)

4.6　25-bar truss optimization

The 25-bar truss structure is shown in Fig. 4-11. There are 8 design variables which are the cross-section areas of the 25 bars, as shown in Table 4-16. The load condition and the design data are listed in Table 4-17. The total weight of 25-bar

41

structure is selected as objective function for weight minimization.
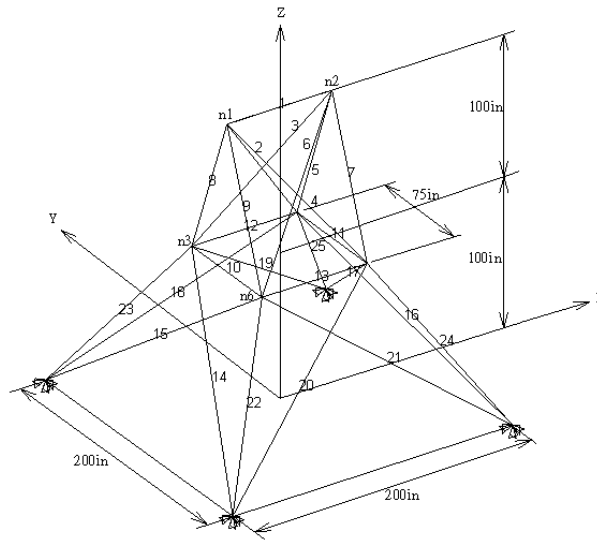
Fig. 4-11 25-bar truss structure

Table 4-16 Selection of design variables of 25-bar optimization

Design variables	x_1	x_2	x_3	x_4	x_5	x_6	x_7	x_8
Element number	1	2,3,4,5	6,7,8,9	10,11	12,13	14,15, 16,17	18,19, 20,21	22,23, 24,25

Table 4-17 Design data for 25-bar truss optimization

Material property		$E = 10000ksi, \ \rho = 0.1lb / in^3, \ v = 0.29$
Load case 1	Node 1	$P_x = 1kips, \ P_y = 10kips, \ P_z = -5kips$
	Node 2	$P_y = 10kips, \ P_z = -5kips$
	Node 3	$P_x = 0.5kips$
	Node 6	$P_x = 0.5kips$
Load case 2	Node 1	$P_y = 20kips, \ P_z = -5kips$
	Node 2	$P_y = -20kips, \ P_z = -5kips$
Constraint of all members	Stress	$-40ksi < \sigma_i < 40ksi$ for each bar
	Displacement	$u_x, u_y, u_z \leq 0.35 \ in$ for node 1~6
	Size	$0.001 \ in^2 \leq x_i \leq 50 \ in^2, i = 1, 2, ..., 8$
	Move limit	$0.25x_i^{(k-1)} \leq x_i^{(k)} \leq 0.75x_i^{(k-1)}, \ i = 1, 2, ..., 8$
Initial design		$x_i = 2.0 \ in^2, \ i = 1, 2, ..., 8$

42

The CPU time for the optimization process is 82 seconds. Conservative approximation is adopted to construct the single-point approximate functions for the initial design. The SAO result of TPPAA is shown in Table 4-18 and Fig. 4-12, and the comparison with previous approximation methods is shown in Table 4-19. In this case, the additional converge criterion is introduced that the relative difference of the design variable in two consecutive iterations is required to be less than 1%.

Table 4-18 Result of TPPAA in 25-bar optimization

|	x_1	x_2	x_3	x_4	x_5	x_6	x_7	x_8	Weight (lb)
Initial design	2.000	2.000	2.000	2.000	2.000	2.000	2.000	2.000	661.44
Iteration 1	0.500	2.013	2.829	0.500	0.500	0.760	1.740	2.821	576.42
Iteration 2	0.125	2.030	3.216	0.125	0.125	0.512	1.549	2.792	546.45
Iteration 3	0.031	2.053	3.051	0.031	0.031	0.694	1.592	2.649	545.77
Iteration 4	0.008	2.025	2.983	0.008	0.008	0.685	1.647	2.668	544.92
Iteration 5	0.002	2.036	3.010	0.002	0.002	0.684	1.625	2.669	544.76
Iteration 6	0.001	2.037	3.007	0.001	0.001	0.685	1.626	2.669	544.73
Optimum design	0.001	2.037	3.007	0.001	0.001	0.685	1.626	2.669	544.73
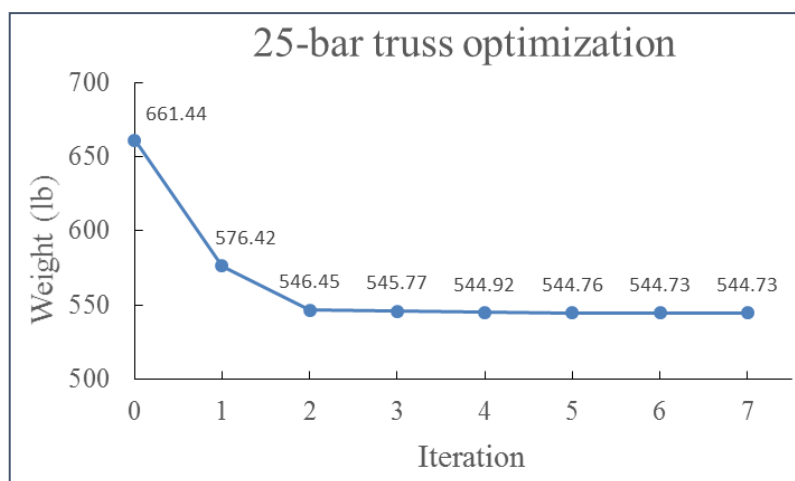
Fig. 4-12 Iteration history of weight of 25-bar truss

43

Table 4-19 Result comparison for 25-bar optimization

Approximation method	Iterations	Weight (lb)
TPPAA	7	544.73
TPPAA (large δ)	7	544.74
TPEA-GBMMA [27]	5	545.74*
ETPEA1 [28]	5	544.78*

(*: premature convergence)
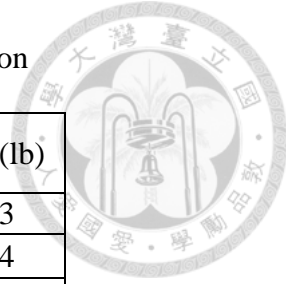
4.7   Multi-section circular beam optimization

The structure of multi-section circular beam is shown in Fig. 4-13. It consists of 10 circular beam elements with the same length. The design data are listed in Table 4-20. A static loading is exerted at the end of this cantilever beam. Total weight is selected as objective function for the purpose of minimizing the weight of beam structure and the diameter D of each beam section is selected as design variables.

Fig. 4-13 Multi-section circular beam structure

Table 4-20 Design data for multi-section circular beam optimization

Material property		$E = 30000\ ksi,\ \rho = 0.1\ lb/in^3,\ \nu = 0.29$
Constraints	Stress	$-1.0\ Mpsi \leq \sigma_i \leq 1.0\ Mpsi,\ i = 1, 2, ..., 10$
	Move limit	$\dfrac{x_i^{(k-1)}}{2.5} \leq x_i^{(k)} \leq 2.5 x_i^{(k-1)},\ i = 1, 2, ..., 10$
Initial design		$x_i = 2.5\ in,\ i = 1, 2, ..., 10$

44

The CPU time for the optimization process is 70 seconds. Conservative approximation is adopted to construct the single-point approximate functions for the initial design. The SAO result with TPPAA is shown in Table 4-21 and Fig. 4-14. The comparison with previous approximation methods is shown in Table 4-22.

Table 4-21 Result of TPPAA in multi-section circular beam optimization

	x_1	x_2	x_3	x_4	x_5	x_6	x_7	x_8	x_9	x_{10}	Weight (lb)
Initial design	2.500	2.500	2.500	2.500	2.500	2.500	2.500	2.500	2.500	2.500	4.9087
Iteration 1	2.481	2.391	2.288	2.167	2.025	1.854	1.646	1.387	1.054	1.000	2.8342
Iteration 2	2.481	2.396	2.304	2.203	2.093	1.970	1.831	1.673	1.512	1.161	3.1500
Iteration 3	2.481	2.396	2.304	2.203	2.093	1.969	1.828	1.661	1.457	1.152	3.1312
Optimum design	2.481	2.396	2.304	2.203	2.093	1.969	1.828	1.661	1.451	1.152	3.1299
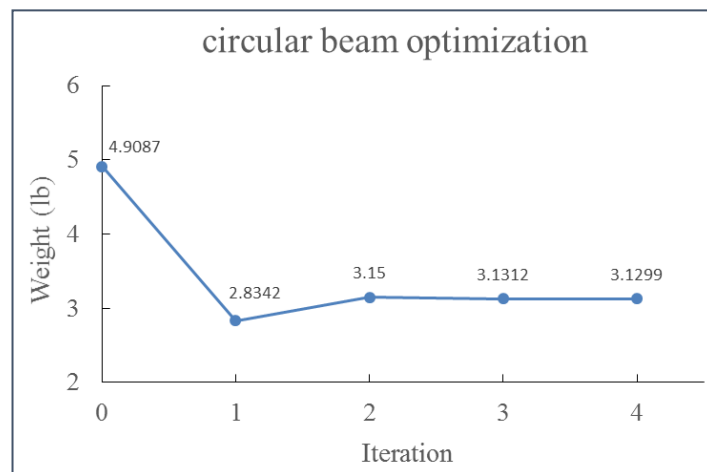
Fig. 4-14 Iteration history of weight of multi-section circular beam

Table 4-22 Result comparison for multi-section circular beam optimization

Approximation method	Iterations	Weight (lb)
TPPAA	4	3.1299
TPEA	3	3.1299
CONLIN	4	3.1299
Direct linear	5	3.1300
TPEA-GBMMA [27]	3	3.1293
ETPEA1 [28]	3	3.1299

45
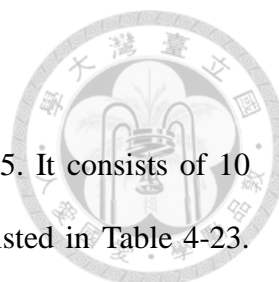
4.8　Multi-section tube beam optimization

The structure of multi-section tube beam is shown in Fig. 4-15. It consists of 10 tubular beam elements with the same length. The design data are listed in Table 4-23. The ratio of outer diameter D to the thickness of the tube T is constant (D/T=12). A static loading is exerted at the end of this cantilever beam. Total weight is selected as objective function for the purpose of minimizing the weight of beam structure and the diameter D of each beam section is selected as design variable.
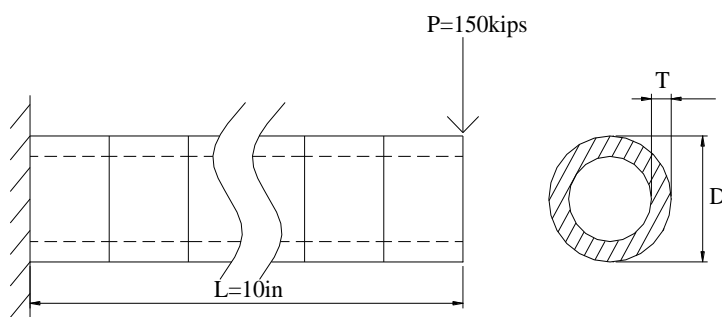
Fig. 4-15 Multi-section tube beam structure

Table 4-23 Design data for multi-section tube beam optimization

Material property		$E = 30000\ ksi,\ \rho = 0.1\ lb/in^3,\ \nu = 0.29$
Constraints	Stress	$-1.0\ Mpsi \le \sigma_i \le 1.0\ Mpsi,\ i = 1,2,...,10$
	Move limit	$\dfrac{x_i^{(k-1)}}{1.8} \le x_i^{(k)} \le 1.8x_i^{(k-1)},\ i = 1,2,...,10$
Initial design		$x_i = 3.6\ in,\ i = 1,2,...,10$

The CPU time for the optimization process is 68 seconds. Conservative approximation is adopted to construct the single-point approximate functions for the initial design. The SAO result of TPPAA is shown in Table 4-24 and Fig. 4-16 respectively. The comparison with previous approximation methods is shown in Table 4-25.

46

Table 4-24 Result of TPPAA in multi-section tube beam optimization

	x_1	x_2	x_3	x_4	x_5	x_6	x_7	x_8	x_9	x_{10}	Weight (lb)
Initial design	3.600	3.600	3.600	3.600	3.600	3.600	3.600	3.600	3.600	3.600	3.1102
Iteration 1	3.016	2.875	2.716	2.536	2.330	2.092	2.000	2.000	2.000	2.000	1.3674
Iteration 2	3.090	2.984	2.869	2.746	2.611	2.465	2.285	2.069	1.777	1.111	1.4643
Iteration 3	3.090	2.984	2.869	2.744	2.606	2.453	2.277	2.069	1.807	1.454	1.4846
Optimum design	3.090	2.984	2.869	2.744	2.606	2.453	2.277	2.069	1.807	1.435	1.4833
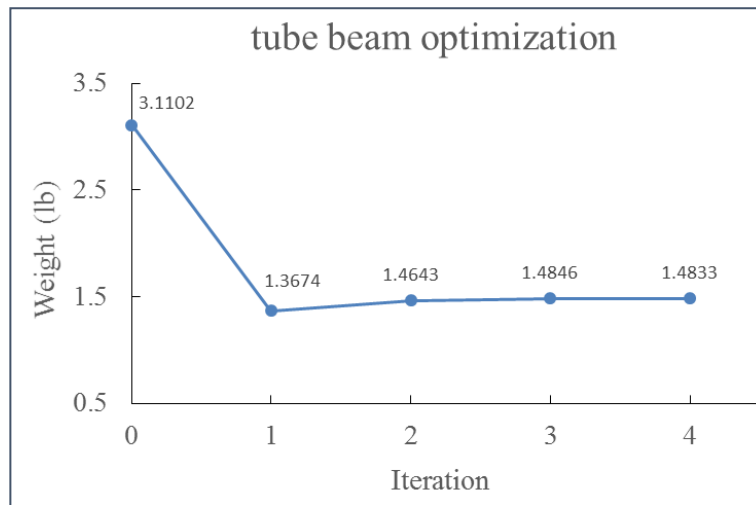
Fig. 4-16 Iteration history of weight of multi-section tube beam

Table 4-25 Result comparison for multi-section tube beam optimization

Approximation method	Iterations	Weight (lb)
TPPAA	4	1.4833
TPEA	3	1.4832
Linear-reciprocal	4	1.4832
Direct linear	5	1.4832
TPEA-GBMMA [27]	3	1.4831
ETPEA1 [28]	3	1.4832

47
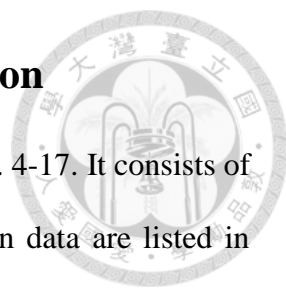
4.9　Multi-section rectangular beam optimization

The structure of multi-section rectangular beam is shown in Fig. 4-17. It consists of 10 rectangular beam elements with the same length, and the design data are listed in Table 4-26. The ratio of rectangular height H to the width W is constant (H/W=3). A static loading is exerted at the end of this cantilever beam. Total weight is selected as objective function for the purpose of minimizing the weight of beam structure and the height H of each beam section is selected as the design variable.
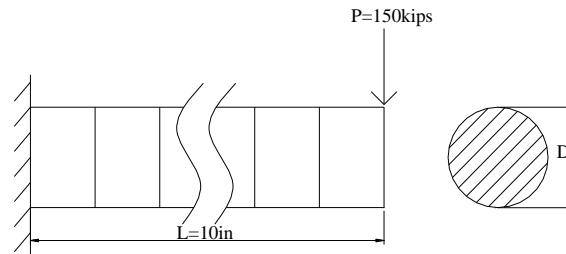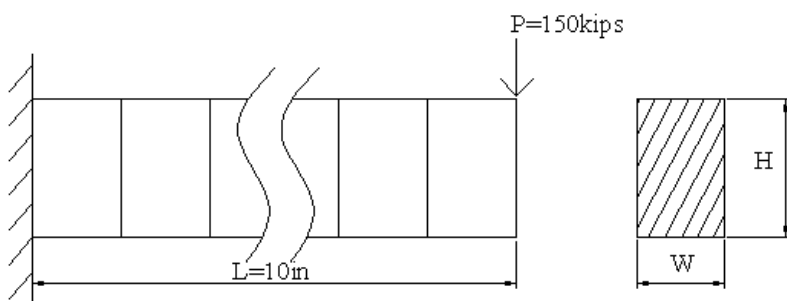

Fig. 4-17 Multi-section rectangular beam structure

Table 4-26 Design data for multi-section rectangular beam optimization

Material property		$E = 30000\ ksi,\ \rho = 0.1\ lb/in^3,\ \nu = 0.29$
Constraints	Stress	$-1.0\ Mpsi \leq \sigma_i \leq 1.0\ Mpsi,\ i = 1, 2, ..., 10$
	Move limit	$\dfrac{x_i^{(k-1)}}{2.5} \leq x_i^{(k)} \leq 2.5 x_i^{(k-1)},\ i = 1, 2, ..., 10$
Initial design		$x_i = 3.0\ in,\ i = 1, 2, ..., 10$

The CPU time for the optimization process is 70 seconds. Conservative approximation is adopted for the approximation of the initial design. The SAO result of TPPAA is shown in Table 4-27 and Fig. 4-18, and the comparison with previous approximation methods is shown in Table 4-28.
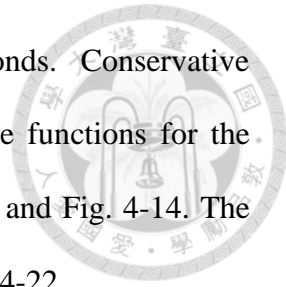
48

Table 4-27 Result of TPPAA in multi-section rectangular beam optimization

	x_1	x_2	x_3	x_4	x_5	x_6	x_7	x_8	x_9	x_{10}	Weight (lb)
Initial design	3.000	3.000	3.000	3.000	3.000	3.000	3.000	3.000	3.000	3.000	3.0000
Iteration 1	1.765	2.893	2.769	2.625	2.455	2.250	2.000	1.688	1.286	1.200	1.7653
Iteration 2	1.953	2.896	2.785	2.664	2.530	2.382	2.213	2.021	1.822	1.405	1.9532
Iteration 3	1.942	2.896	2.785	2.664	2.530	2.381	2.210	2.008	1.760	1.393	1.9423
Optimum design	1.942	2.896	2.785	2.664	2.530	2.381	2.210	2.008	1.754	1.392	1.9416
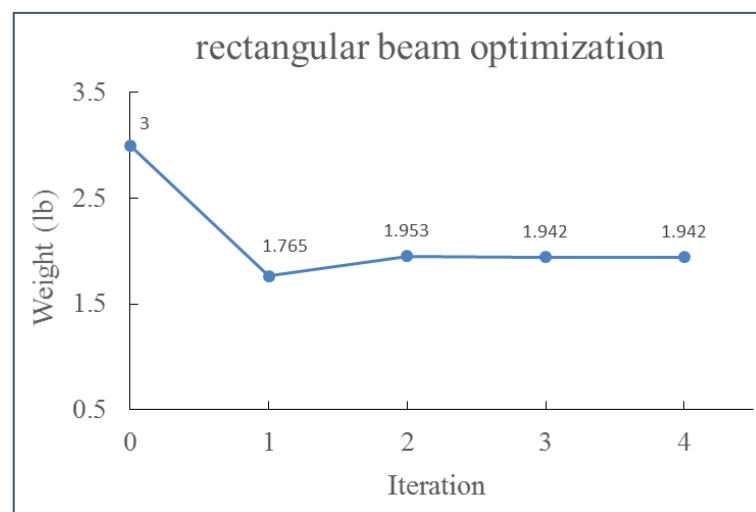
Fig. 4-18 Iteration history for multi-section rectangular beam

Table 4-28 Result of multi-section rectangular beam

Approximation method	Iterations	Weight (lb)
TPPAA	4	1.9416
TPEA	3	1.9416
Linear-reciprocal	4	1.9416
Direct linear	5	1.9416
TPEA-GBMMA [27]	3	1.9418
ETPEA1 [28]	3	1.9418

49

Chapter 5   Optimization of large scale structures
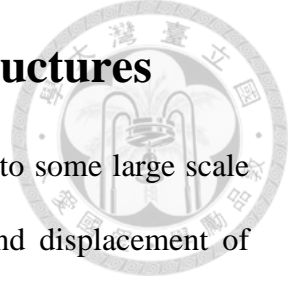
In this chapter, the proposed approximation scheme is applied to some large scale structures for verifying its practicability. The natural frequency and displacement of structures are approximated as explicit functions for structural optimization in this chapter. The specifications of computer used for the examples in this chapter is Intel i7-6700 3.40GHz CPU with 16GB DDR4-2133 RAM

5.1   Effective finite element model construction for PCB

Dynamic analysis is crucial in the design of PCB because vibration can affect the life cycle of PCB [29][30]. Through FEA, it is efficient to design PCB with considering its dynamic characteristics. However, since PCB consists of several materials, it is not practical to construct the complicate non-homogeneous FE model. Instead, the anisotropic homogeneous FE model is constructed according to the natural frequencies obtained by experimental modal analysis (EMA).

Herein, the effective FE model for a glass fiber board is assumed to be the orthotropic material. The strain-stress relation can be expressed as

$$
\begin{bmatrix} \varepsilon_x \\ \varepsilon_y \\ \varepsilon_z \\ \gamma_{xy} \\ \gamma_{yz} \\ \gamma_{xz} \end{bmatrix} = \begin{bmatrix} \dfrac{1}{E_x} & \dfrac{-\nu_{yx}}{E_y} & \dfrac{-\nu_{zx}}{E_z} & 0 & 0 & 0 \\ \dfrac{-\nu_{xy}}{E_x} & \dfrac{1}{E_y} & \dfrac{-\nu_{yz}}{E_z} & 0 & 0 & 0 \\ \dfrac{-\nu_{xz}}{E_x} & \dfrac{-\nu_{yz}}{E_y} & \dfrac{1}{E_z} & 0 & 0 & 0 \\ 0 & 0 & 0 & \dfrac{1}{G_{xy}} & 0 & 0 \\ 0 & 0 & 0 & 0 & \dfrac{1}{G_{yz}} & 0 \\ 0 & 0 & 0 & 0 & 0 & \dfrac{1}{G_{xz}} \end{bmatrix} \begin{bmatrix} \sigma_x \\ \sigma_y \\ \sigma_z \\ \tau_{xy} \\ \tau_{yz} \\ \tau_{xz} \end{bmatrix}. \tag{5.1}
$$

The aim of this optimization problem is to find the least squared error of frequencies between effective FE model and EMA result, hence the objective function $f(\bar{x})$ is expressed as

$$f(\bar{x}) = \sum_{i=1}^{n_f} \left(\frac{h_i(\bar{x}) - \tilde{h}_i}{\tilde{h}_i} \right)^2 \tag{5.2}$$

where $h_i(\bar{x})$ denotes the *i*-th frequency of approximate function with elastic constants to be design variables, $\tilde{h}_i$ denotes the *i*-th frequency of EMA result, n_f denotes the number of the measured frequencies from EMA.

5.1.1 Material property identification for orthotropic thin plate

Before constructing the effective FE model for real PCB, to test the accuracy of this optimization program without considering the error of FEA, identifying the elastic constants of an orthotropic plate by fitting natural frequencies from FEA is presented first. The thin plate is a cuboid with length 70 mm, width 50 mm, and thick 1 mm, and the coordinate is shown in Fig. 5-1. Fitting the frequencies from two boundary conditions and is adopted herein. One is the free-free boundary condition, and the other is fixing the surface at $x=0$. The material property of this thin plate is listed in Table 5-1. The element size is 2 mm with solid 45. The meshed FE model of this thin plate is shown in Fig. 5-2, and the natural frequencies are listed in Table 5-2.

Fig. 5-1 CAD model of the thin plate

51

Table 5-1 Material property of the thin plate

Material property	
E_x	10 GPa
E_y	30 GPa
E_z	25 GPa
G_{xy}	7 GPa
G_{yz}	5 GPa
G_{xz}	5 GPa
v_{xy}	0.15
v_{yz}	0.15
v_{xz}	0.15
ρ	5 g/cm^3
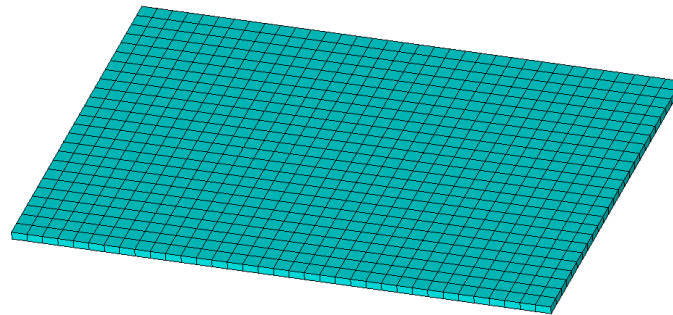
Fig. 5-2 Meshed FE model of thin plate

Table 5-2 Natural frequencies of the thin plate

Free-free (Hz)		Fixed at $x = 0$ (Hz)	
Mode 1	298.087	Mode 1	47.5430
Mode 2	347.715	Mode 2	194.984
Mode 3	769.697	Mode 3	296.941
Mode 4	827.398	Mode 4	637.830
Mode 5	1033.07	Mode 5	833.642
Mode 6	1257.34	Mode 6	1104.69
Mode 7	1351.69	Mode 7	1238.64

For a thin plate, only 4 of the 9 independent elastic constants in orthotropic material affects the natural frequencies. These 4 elastic constants are selected as design

52

variables for fitting the natural frequencies, as shown in Table 5-3. The design data is shown in Table 5-4.

Table 5-3 Selection of design variables for fitting the frequencies of the thin plate

Design variable	x_1	x_2	x_3	x_4
Elastic constant	E_x	E_y	G_{xy}	v_{xy}

(unit: GPa for $x_1 \sim x_3$)

Table 5-4 Design data for fitting natural frequencies of the thin plate

Constraints	Side	$-1 \leq x_4 \leq 0.5$
	Move limit	$0.5 x_i^{(k-1)} \leq x_i^{(k)} \leq 1.5 x_i^{(k-1)},\ i = 1, 2, 3$ $x_4^{(k-1)} - 0.05 \leq x_4^{(k)} \leq x_4^{(k-1)} + 0.05$
Initial design		$x_1 = 20,\ x_2 = 20,\ x_3 = 20,\ x_4 = 0.2$

The CPU time for the optimization process is 126 seconds. Direct linear approximation is adopted to construct the single-point approximate functions for the initial design. The result indicates that both the frequencies and elastic constants can be fit accurately, as shown in Table 5-5 and Table 5-6. The SAO result of TPPAA is shown in Table 5-7.

53

Table 5-5 Result of natural frequencies after fitting

	Free-free	
	After fitting (Hz)	Aim (Hz)
Mode 1	298.087	298.087
Mode 2	347.715	347.715
Mode 3	769.697	769.697
Mode 4	827.398	827.398
Mode 5	1033.07	1033.07
Mode 6	1257.34	1257.34
Mode 7	1351.69	1351.69
	Fixed at $x = 0$	
	After fitting (Hz)	Aim (Hz)
Mode 1	47.5430	47.5430
Mode 2	194.984	194.984
Mode 3	296.941	296.941
Mode 4	637.830	637.830
Mode 5	833.642	833.642
Mode 6	1104.69	1104.69
Mode 7	1238.64	1238.64

Table 5-6 Obtained elastic constants by fitting natural frequencies

Elastic constant	Aim	After fitting
E_x (GPa)	10	10.0000
E_y (GPa)	30	30.0000
G_{xy} (GPa)	7	7.0000
ν_{xy}	0.15	0.1500

Table 5-7 Result of TPPAA in elastic constants identification of the thin plate

	x_1	x_2	x_3	x_4	Squared error
Initial design	20.00	20.00	20.00	0.200	2.5E1
Iteration 1	10.00	15.77	10.00	0.150	2.6E-1
Iteration 2	9.949	18.63	8.065	0.200	1.2E-1
Iteration 3	9.834	24.32	6.892	0.259	6.7E-2
Iteration 4	9.651	27.48	6.928	0.209	4.6E-3
Iteration 5	9.992	29.90	6.989	0.159	4.1E-3
Iteration 6	10.00	30.00	7.000	0.150	4.7E-6
Iteration 7	10.00	30.00	7.000	0.150	6E-11
Iteration 8	10.00	30.00	7.000	0.150	1E-16
Optimum design	10.00	30.00	7.000	0.150	1E-16

54
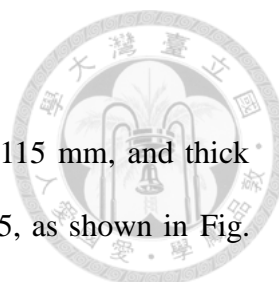
5.1.2 Effective FE model construction for PCB

This glass fiber PCB is a cuboid with length 165 mm, width 115 mm, and thick 1.53 mm. The element size of meshed model is 2 mm with solid 45, as shown in Fig. 5-3. The two boundary conditions for natural frequencies and the coordinate are shown in Fig. 5-4.
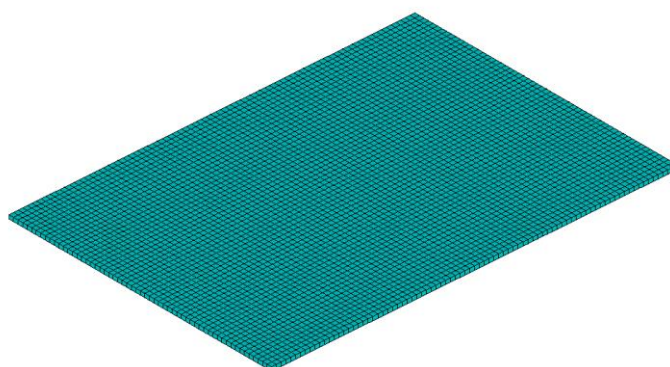
Fig. 5-3 Meshed FE model of PCB
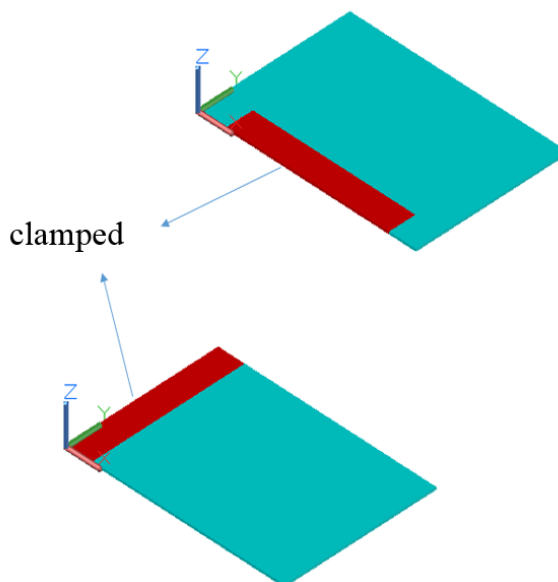
Fig. 5-4 Boundary conditions for EMA of PCB

The natural frequencies of PCB is obtained from EMA, as shown in Fig. 5-5. The result of EMA is listed in Table 5-8

55
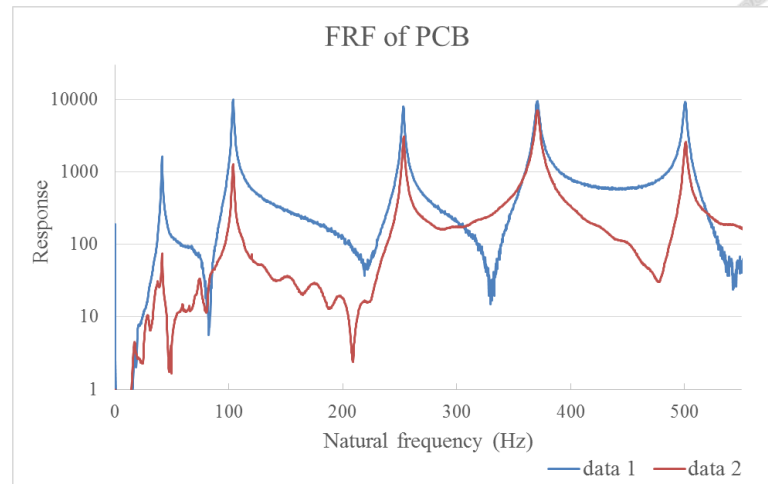
Fig. 5-5 FRF of PCB by EMA

Table 5-8 EMA result of PCB

Clamped at the long side (Hz)		Clamped at the short side (Hz)	
Mode 1	92.7	Mode 1	41.5
Mode 2	136	Mode 2	104
Mode 3	300	Mode 3	253
Mode 4	540	Mode 4	371
Mode 5	591		
Mode 6	700		

The elastic constants which affect the natural frequencies are selected as design variables for effective FE model construction, as shown in Table 5-9. The other material properties are list in Table 5-10. The design data is shown in Table 5-11.

Table 5-9 Selection of design variables for fitting natural frequencies of the PCB

Design variable	x_1	x_2	x_3	x_4
Elastic constant	E_x	E_y	G_{xy}	v_{xy}

(unit: GPa for $x_1 \sim x_3$)

56

Table 5-10 Material properties of PCB

Material property	
E_z (GPa)	20
G_{yz} (GPa)	7.69
G_{xz} (GPa)	7.69
v_{yz}	0.3
v_{xz}	0.3
ρ (g/cm^3)	2

Table 5-11 Design data for effective FE model

Constraints	Side	$-1 \leq x_4 \leq 0.5$
	Move limit	$0.8 x_i^{(k-1)} \leq x_i^{(k)} \leq 1.2 x_i^{(k-1)}, \; i = 1, 2, 3$ $x_4^{(k-1)} - 0.05 \leq x_4^{(k)} \leq x_4^{(k-1)} + 0.05$
Initial design		$x_1 = 15, x_2 = 15, x_3 = 6.8, x_4 = 0.1$

The CPU time for the optimization process is 142 seconds. Direct linear approximation is adopted to construct the single-point approximate functions for the initial design. The result indicates that the frequencies of a glass fiber PCB can be fit well that the max difference of the natural frequencies between FEA and EMA is in 4% by orthotropic material model, as shown in Table 5-12. The SAO result with TPPAA is shown in Table 5-13. The comparison with other approximation methods are also presented to verify the solution as listed in Table 5-14.

57

Table 5-12 Comparison of natural frequencies between effective model and EMA result

Clamped at the long side			
	After fitting (Hz)	Aim (Hz)	Difference (%)
Mode 1	91.27	92.7	1.5
Mode 2	136.7	136	0.5
Mode 3	294.3	300	1.9
Mode 4	561.7	540	4.0
Mode 5	571.5	591	3.3
Mode 6	678.3	700	3.1
Clamped at the short side			
	After fitting (Hz)	Aim (Hz)	Difference (%)
Mode 1	41.62	41.5	0.3
Mode 2	104.6	104	0.6
Mode 3	257.3	253	1.7
Mode 4	379.1	371	2.2

Table 5-13 SAO result with TPPAA for PCB FE model construction

	x_1	x_2	x_3	x_4	Squared error
Initial design	15.00	15.00	6.818	0.100	2.4E-1
Iteration 1	18.00	18.00	7.683	0.150	7.9E-2
Iteration 2	21.60	21.60	6.600	0.200	1.4E-2
Iteration 3	23.99	21.76	6.061	0.250	5.4E-3
Iteration 4	23.71	21.33	6.039	0.300	5.2E-3
Iteration 5	23.51	21.05	6.030	0.325	5.1E-3
Iteration 6	23.51	21.04	6.029	0.326	5.1E-3
Optimum design	23.50	21.04	6.029	0.326	5.1E-3

Table 5-14 Result comparison with different approximation methods

Approximation method	x_1	x_2	x_3	x_4	Squared error	Iteration
TPPAA	23.50	21.04	6.029	0.326	5.1E-3	7
DQA	23.50	21.04	6.029	0.326	5.1E-3	7
Direct linear	23.50	21.04	6.029	0.326	5.1E-3	8

58

5.2   Optimization of high-accuracy measuring stage

Recently, since the semiconductor is developed to be smaller, faster, lower power consuming and higher circuit-density, the demand for precision positioning technique increases rapidly. Herein, the optimization of measuring stage for wafer inspection is presented, as shown in Fig. 5-6 which minimizes the weight and ensures positioning accuracy against the structure deformation caused by static loading and vibration at the same time.
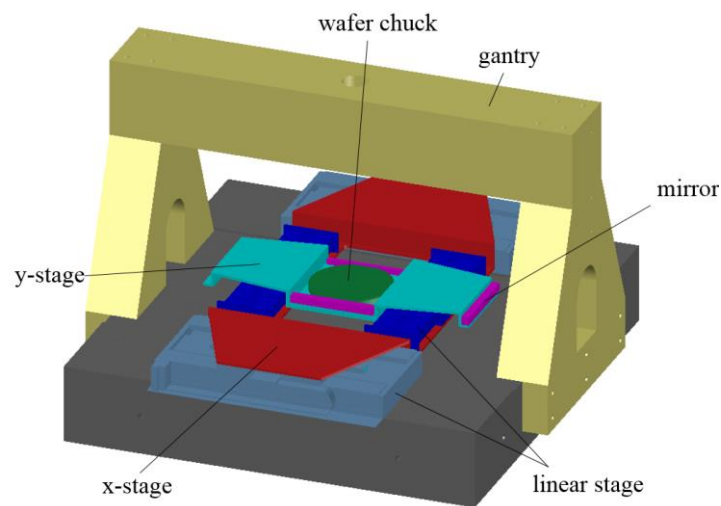
Fig. 5-6 High-accuracy measuring stage for wafer inspection

5.2.1   Optimization of gantry

The selection of design variables of gantry is shown in Fig. 5-7. The element size of meshed FE model is 40 mm with hexahedral solid 95. The bottom of the gantry is fixed in FEA as shown in Fig. 5-8. The material properties are shown in Table 5-15.

59
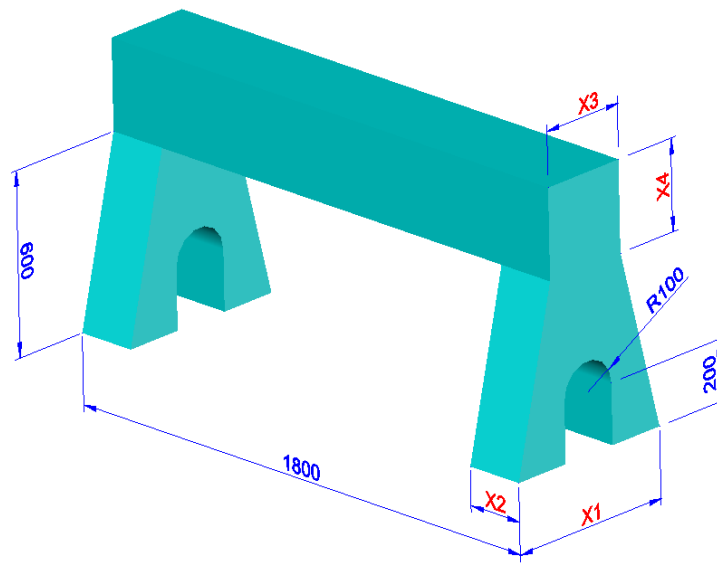
(unit: mm)

Fig. 5-7 Selection of design variables for gantry

fixed at bottom
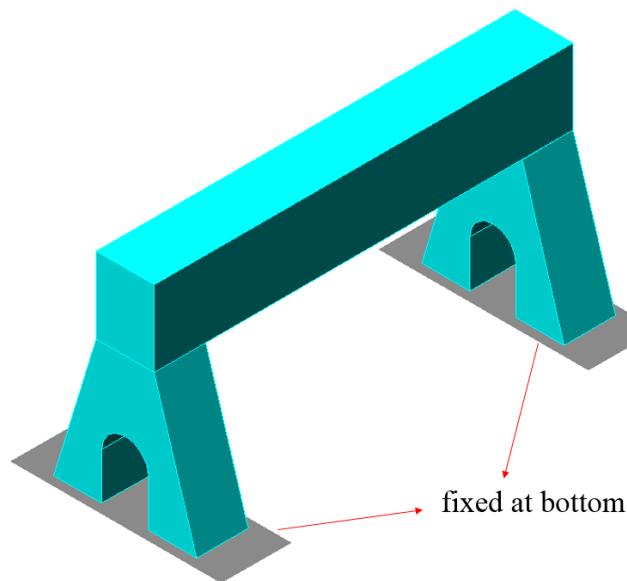
Fig. 5-8 Boundary condition of gantry in FEA

Table 5-15 Material property of gantry

Material	Granite
E (GPa)	60
v	0.3
ρ (g/cm^3)	2.66
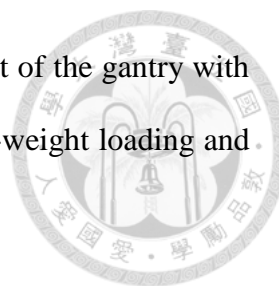
60

The goal of this optimization problem is to minimize the weight of the gantry with considering the restriction of the maximum displacement under self-weight loading and 1st natural frequency. The design data is shown in Table 5-16.

Table 5-16 Design data of gantry optimization

Constraints	Size		$550 < x_1 < 800$ $100 < x_2 < 220$ $250 < x_3 < 500$ $100 < x_4 < 400$
	Move limit		$0.7 x_i^{(k-1)} \leq x_i^{(k)} \leq 1.3 x_i^{(k-1)}, \; i = 1, 2, 3, 4$
	Behavior	Case A	Max displacement < 3 μm
		Case B	1st frequency > 220 Hz
		Case C	Max displacement < 3 μm 1st frequency > 220 Hz
Initial design			$x_1 = 700, \; x_2 = 200, \; x_3 = 270, \; x_4 = 250$

The SAO result with TPPAA is shown in Table 5-17, Table 5-18, Table 5-19 and Fig. 5-9. The CPU time is 74 seconds in case A, 254 seconds in case B and 133 seconds in case C. Direct linear approximation is adopted to construct the single-point approximate functions for the initial design. The comparison of results with different approximation methods is shown in Table 5-20, Table 5-21 and Table 5-22.

Table 5-17 Result of TPPAA for gantry optimization in case A

	x_1	x_2	x_3	x_4	weight (kgf)
Initial design	700.0	200.0	270.0	250.0	594.8
Iteration 1	550.0	220.0	250.0	243.7	530.8
Iteration 2	550.0	220.0	250.0	240.0	526.3
Optimum design	550.0	220.0	250.0	240.1	526.6

61

Table 5-18 Result of TPPAA for gantry optimization in case B

	x_1	x_2	x_3	x_4	weight (kgf)
Initial design	700.0	200.0	270.0	250.0	594.8
Iteration 1	636.1	220.0	250.0	175.0	478.8
Iteration 2	583.1	220.0	250.0	122.5	397.4
Iteration 3	550.0	217.5	250.0	101.7	358.1
Iteration 4	550.0	216.7	250.0	105.4	361.7
Optimum design	550.0	216.8	250.0	105.6	362.1

Table 5-19 Result of TPPAA for gantry optimization in case C

	x_1	x_2	x_3	x_4	weight (kgf)
Initial design	700.0	200.0	270.0	250.0	594.8
Iteration 1	707.5	220.0	250.0	229.0	568.5
Iteration 2	696.0	220.0	250.0	225.9	560.7
Optimum design	695.8	220.0	250.0	225.9	560.7
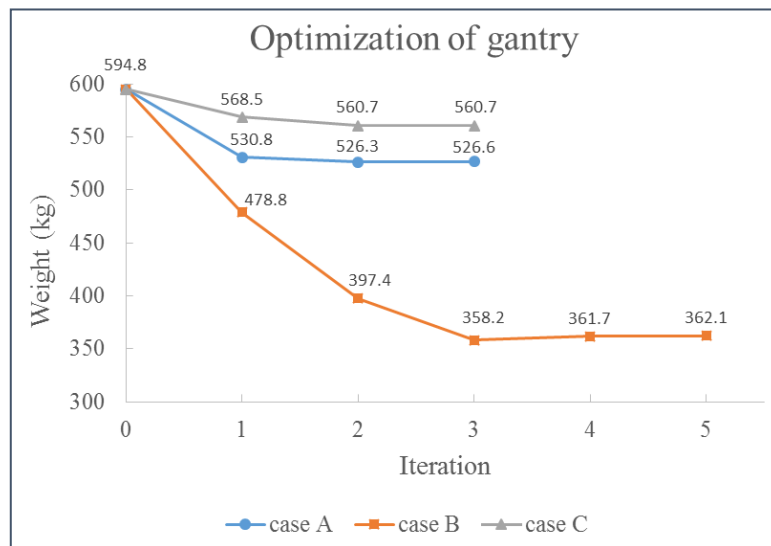
Fig. 5-9 Iteration history of weight of gantry

Table 5-20 Result comparison of gantry optimization in case A

Approximation method	x_1	x_2	x_3	x_4	weight (kgf)	max disp. (μm)	Iteration
TPPAA	550.0	220.0	250.0	240.1	526.6	3.00	3
TPEA	550.0	220.0	250.0	240.1	526.5	3.00	3
Direct linear	550.0	220.0	250.0	240.0	526.4	3.00	3

Table 5-21 Result comparison of gantry optimization in case B

Approximation method	x_1	x_2	x_3	x_4	weight (kgf)	1st N.F. (Hz)	2nd N.F. (Hz)	Iteration
TPPAA	550.0	216.8	250.0	105.6	362.1	220	220	5
TPEA	550.0	216.8	250.0	105.6	362.0	220	220	5
DQA	550.0	216.8	250.0	105.6	362.1	220	220	5
Direct linear	550.0	216.8	250.0	105.7	362.1	220	220	5

Table 5-22 Result comparison of gantry optimization in case C

Approximation method	x_1	x_2	x_3	x_4	weight (kgf)	1st N.F. (Hz)	max disp. (μm)	Iteration
TPPAA	695.8	220.0	250.0	225.9	560.7	220	3.00	3
TPEA	695.7	220.0	250.0	225.9	560.7	220	3.00	3
Direct linear	695.9	220.0	250.0	225.9	560.8	220	3.00	3

5.2.2 Optimization of modified gantry

The selection of design variables of the modified gantry is shown in Fig. 5-10. The element size of meshed model is 40 mm with solid 186 tetrahedral and hexahedral element mixed as shown in Fig. 5-11. The boundary condition and the material property remain the same as original gantry.

63
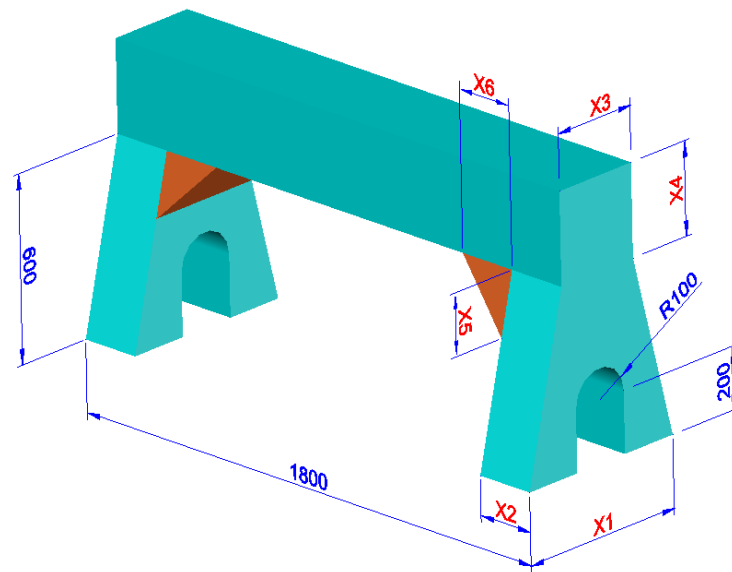
(unit: mm)
Fig. 5-10 Selection of design variables for modified gantry

.
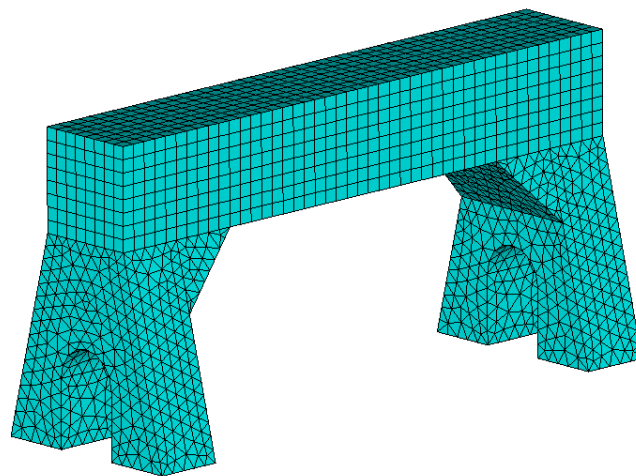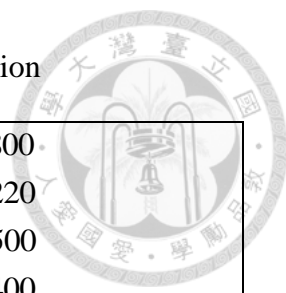
Fig. 5-11 Meshed FE model of modified gantry

The goal of this optimization problem is to minimize the weight of the gantry with considering the restriction of the maximum displacement under self-weight loading and 1st natural frequency. The design data is shown in Table 5-23.

Table 5-23 Design data of modified gantry optimization

Constraints	Size	Case A	$550 < x_1 < 800$
			$100 < x_2 < 220$
			$250 < x_3 < 500$
			$100 < x_4 < 400$
			$100 < x_5 < 250$
			$100 < x_6 < 300$
		Case B	$550 < x_1 < 800$
			$100 < x_2 < 200$
			$250 < x_3 < 500$
			$50 < x_4 < 400$
			$100 < x_5 < 250$
			$100 < x_6 < 300$
	Move limit		$0.85x_i^{(k-1)} \le x_i^{(k)} \le 1.15x_i^{(k-1)},\ i=1,2,...,6$
	Behavior	Case A	Max displacement $< 3\ \mu m$ 1st natural frequency > 220 Hz
		Case B	Max displacement $< 3\ \mu m$ 1st natural frequency > 235 Hz
Initial design	Case A		$x_1 = 700,\ x_2 = 200,\ x_3 = 270,$ $x_4 = 250,\ x_5 = 200,\ x_6 = 250$
	Case B		$x_1 = 720,\ x_2 = 190,\ x_3 = 270,$ $x_4 = 210,\ x_5 = 200,\ x_6 = 250$

The SAO result with TPPAA is shown in Table 5-24, Table 5-25, Fig. 5-12 and Fig. 5-13. The CPU time is 700 seconds in case A and 804 seconds in case B. Direct linear approximation is adopted to construct the single-point approximate functions for the initial design in both cases. The comparison of results with different approximation methods is shown in Table 5-26 and Table 5-27.

Table 5-24 Result of TPPAA for modified gantry optimization in case A

	x_1	x_2	x_3	x_4	x_5	x_6	weight (kgf)
Initial design	700.0	200.0	270.0	250.0	200.0	250.0	616.0
Iteration 1	595.0	174.2	250.0	212.5	230.0	286.2	481.9
Iteration 2	550.0	181.0	250.0	180.6	250.0	300.0	442.0
Iteration 3	550.0	191.8	250.0	153.5	239.1	300.0	419.9
Iteration 4	550.0	198.9	250.0	130.5	203.2	300.0	395.4
Iteration 5	550.0	204.4	250.0	110.9	172.7	300.0	374.1
Iteration 6	550.0	205.6	250.0	100.0	146.8	300.0	359.3
Iteration 7	550.0	205.2	250.0	100.0	138.8	300.0	357.9
Optimum design	550.0	205.2	250.0	100.0	138.7	300.0	357.9

Table 5-25 Result of TPPAA for modified gantry optimization in case B

	x_1	x_2	x_3	x_4	x_5	x_6	weight (kgf)
Initial design	720.0	190.0	270.0	210.0	200.0	250.0	556.9
Iteration 1	612.0	199.0	250.0	178.5	170.0	287.5	468.1
Iteration 2	614.2	200.0	250.0	151.7	195.5	300.0	442.1
Iteration 3	673.0	200.0	250.0	129.0	208.8	300.0	435.9
Iteration 4	718.1	200.0	250.0	109.6	198.9	300.0	426.2
Iteration 5	712.1	200.0	250.0	93.18	169.0	300.0	400.4
Iteration 6	721.7	200.0	250.0	79.20	176.9	300.0	387.9
Iteration 7	729.7	200.0	250.0	72.95	196.3	300.0	385.7
Optimum design	726.9	200.0	250.0	73.36	199.8	300.0	385.8
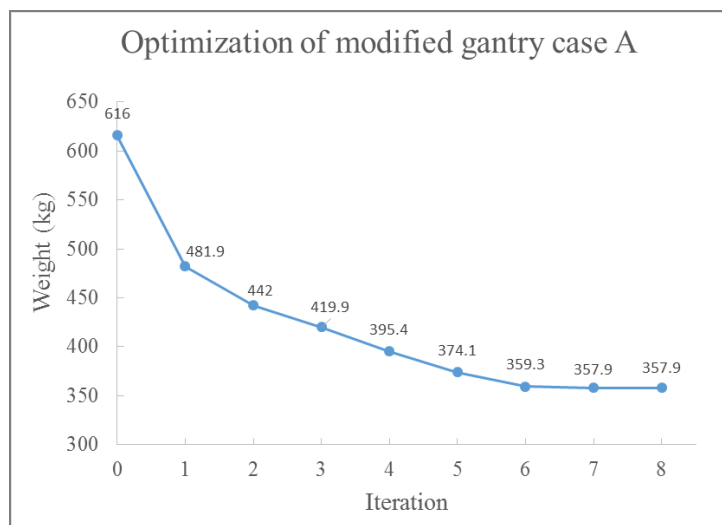
Fig. 5-12 Iteration history of weight of modified gantry in case A

66
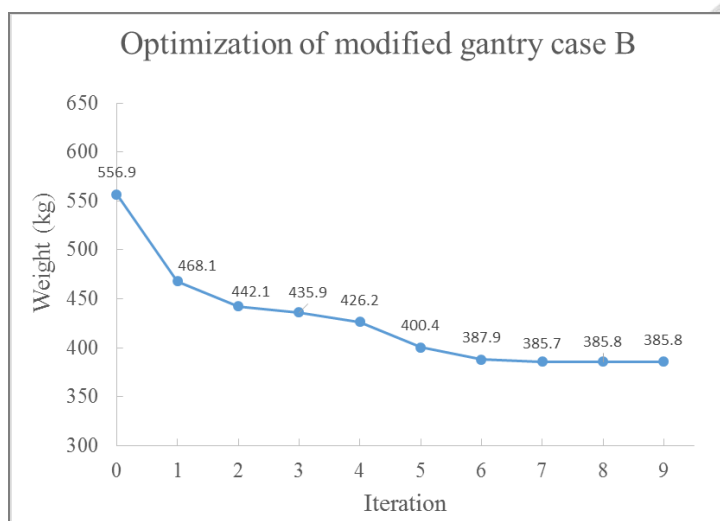
Fig. 5-13 Iteration history of weight of modified gantry in case B

Table 5-26 Result comparison of modified gantry optimization in case A

Approximation method	x_1	x_2	x_3	x_4	x_5	x_6	weight (kgf)	1st N.F. (Hz)	max disp. (μm)	Iteration
TPPAA	550.0	205.2	250.0	100.0	138.7	300.0	357.9	220	3.00	8
TPEA	550.0	205.2	250.0	100.0	138.7	300.0	357.9	220	3.00	8
DQA	550.0	205.2	250.0	100.0	138.6	300.0	357.9	220	3.00	8

Table 5-27 Result comparison of modified gantry optimization in case B

Approximation method	x_1	x_2	x_3	x_4	x_5	x_6	weight (kgf)	1st N.F. (Hz)	max disp. (μm)	Iteration
TPPAA	726.9	200.0	250.0	73.4	199.8	300.0	385.8	235	3.00	9
TPEA	726.4	200.0	250.0	73.7	198.5	300.0	385.8	235	3.00	10
CONLIN	726.3	200.0	250.0	73.8	198.1	300.0	385.8	235	3.00	10

5.2.3 Optimization of y-stage

The simplified parametric CAD model of y-stage for optimization is shown in Fig. 5-14. The thickness of each plate is selected as design variable, as shown in Fig. 5-15. The element type of meshed model is solid 186 with tetrahedral and hexahedral elements mixed as shown in Fig. 5-16. In FEA, the bottom of the linear stage is fixed.

The material property are listed in Table 5-28.

Fig. 5-14 Simplified parametric CAD model of y-stage

(unit: mm)
Fig. 5-15 Selection of design variable for y-stage
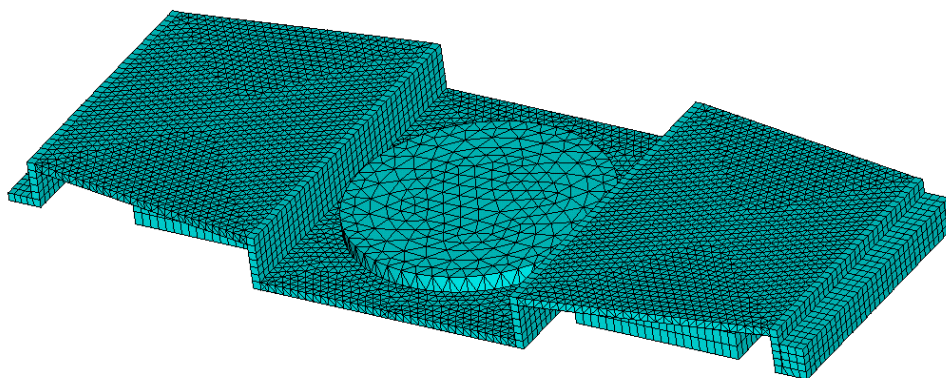
Fig. 5-16 Meshed model of y-stage

68

Table 5-28 Material property of y-stage

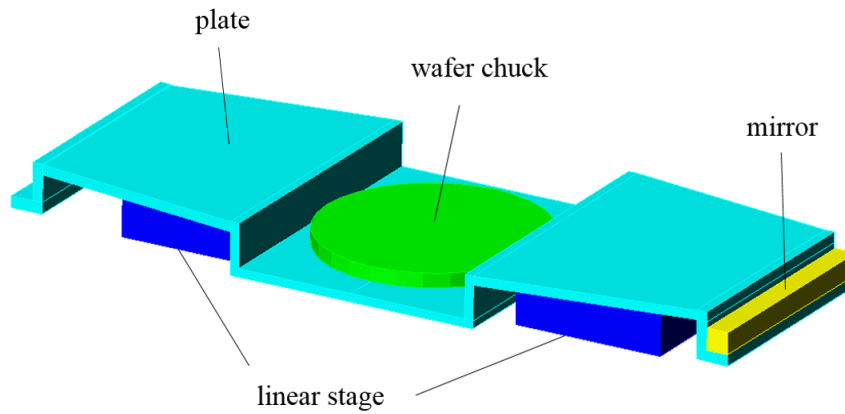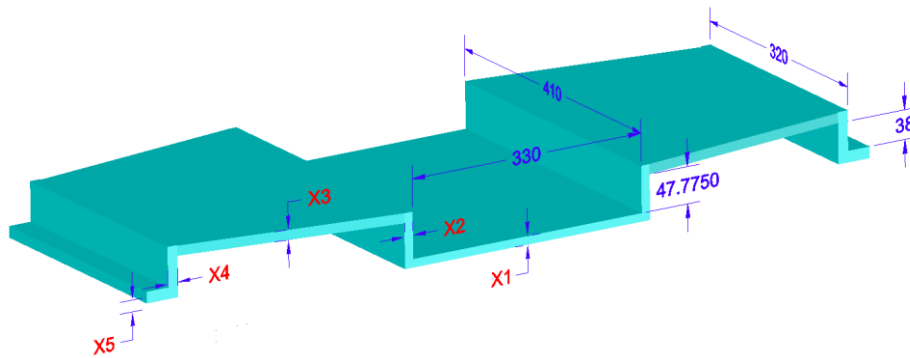| Component	plate	mirror	wafer chuck	linear stage
Material	invar	zerodur	aluminum alloy	aluminum alloy
E (GPa)	150	91	303	68
v	0.3	0.24	0.21	0.33
ρ (g/cm^3)	8	2.53	3.72	3.59

The goal of this optimization problem is to minimize the weight of the y-stage with considering the restriction of the maximum displacement under self-weight loading and 1st natural frequency. The design data is shown in Table 5-29.

Table 5-29 Design data of y-stage optimization

	Size		$3 < x_i < 30, \quad i = 1, 2, ..., 5$
	Move limit		$0.7 x_i^{(k-1)} \leq x_i^{(k)} \leq 1.3 x_i^{(k-1)}, \quad i = 1, 2, ..., 5$
Constraints	Behavior	Case A	Max displacement < 3 μm
		Case B	1st natural frequency > 250 Hz
		Case C	Max displacement < 3 μm 1st natural frequency > 250 Hz
Initial design			$x_i = 10, \quad i = 1, 2, ..., 5$

The SAO result with TPPAA is shown in Table 5-30, Table 5-31, Table 5-32 and Fig. 5-17. The CPU time is 493 seconds in case A, 1224 seconds in case B and 1230 seconds in case C. Direct linear approximation is adopted to construct the single-point approximate functions for the initial design. The comparison of results with different approximation methods is shown in Table 5-33, Table 5-34 and Table 5-35. To examine the optimization result, TPAEA with large δ is also taken in these cases. δ is selected to be large enough so that the convex substitute functions are always adopted for approximation. With larger δ adopted, SAO process can be more stable.

Table 5-30 Result of TPPAA for y-stage optimization in case A

	x_1	x_2	x_3	x_4	x_5	weight (kgf)
Initial design	10.00	10.00	10.00	10.00	10.00	28.59
Iteration 1	7.000	7.000	10.79	7.000	7.000	23.15
Iteration 2	4.900	4.900	11.35	4.900	4.900	19.44
Iteration 3	3.454	3.431	11.38	5.171	3.863	17.14
Iteration 4	3.000	3.000	11.33	5.168	3.000	16.26
Optimum design	3.000	3.000	11.34	5.170	3.000	16.26

Table 5-31 Result of TPPAA for y-stage optimization in case B

	x_1	x_2	x_3	x_4	x_5	weight (kgf)
Initial design	10.00	10.00	10.00	10.00	10.00	28.59
Iteration 1	7.000	7.000	9.168	7.000	7.000	21.60
Iteration 2	4.900	4.900	8.552	4.900	4.900	16.83
Iteration 3	3.430	3.814	8.438	3.567	3.432	14.05
Iteration 4	3.000	3.874	7.858	4.504	3.000	13.22
Iteration 5	3.000	3.871	8.209	4.252	3.037	13.49
Iteration 6	3.000	3.875	8.175	4.243	3.028	13.46
Optimum design	3.000	3.869	8.180	4.242	3.017	13.46

Table 5-32 Result of TPPAA for y-stage optimization in case C

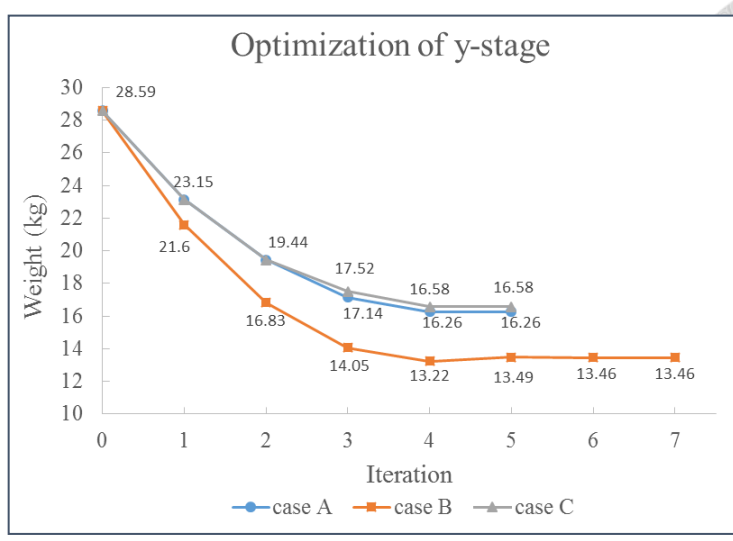|	x_1	x_2	x_3	x_4	x_5	weight (kgf)
Initial design	10.00	10.00	10.00	10.00	10.00	28.59
Iteration 1	7.000	7.000	10.79	7.000	7.000	23.15
Iteration 2	4.900	4.900	11.35	4.900	4.900	19.44
Iteration 3	3.430	4.094	11.55	4.943	4.084	17.52
Iteration 4	3.000	3.712	11.45	4.882	3.000	16.58
Optimum design	3.000	3.724	11.44	4.882	3.000	16.58

Fig. 5-17 Iteration history of weight of y-stage

Table 5-33 Result comparison of y-stage optimization in case A

Approximation method	x_1	x_2	x_3	x_4	x_5	weight (kgf)	max disp. (μm)
TPPAA	3.000	3.000	11.34	5.170	3.000	16.26	3.00
Direct linear *	3.000	3.000	11.35	5.120	3.000	16.26	3.00
TPPAA (large δ)	3.000	3.000	11.39	4.997	3.000	16.27	3.00

(*: different move limit)

Table 5-34 Result comparison of y-stage optimization in case B

Approximation method	x_1	x_2	x_3	x_4	x_5	weight (kgf)	1st N.F. (Hz)	2nd N.F. (Hz)
TPPAA	3.000	3.869	8.180	4.242	3.017	13.46	250	250
TPPAA (large δ)	3.000	3.877	8.194	4.071	3.000	13.43	250	250

Table 5-35 Result comparison of y-stage optimization in case C

Approximation method	x_1	x_2	x_3	x_4	x_5	weight (kgf)	1st N.F. (Hz)	max disp. (μm)	Iteration
TPPAA	3.000	3.724	11.44	4.882	3.000	16.58	250	3.00	5
TPEA	3.000	3.725	11.33	5.181	3.001	16.56	250	3.00	9
TPPAA (large δ)	3.000	3.725	11.33	5.221	3.000	16.56	250	3.00	9

71

Chapter 6   Conclusion and suggestion
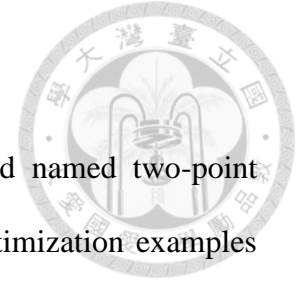
This study proposes a new two-point approximation method named two-point piecewise adaptive approximation (TPPAA). Several structural optimization examples are also presented and show the applicability of this new approximation method. The conclusions and suggestions are listed in this chapter.

6.1   Conclusion

The conclusions of this thesis are expressed as follows:

(1) As a two-point approximation scheme, TPPAA satisfies the function value at the current design point and the gradients at the both design points. To ensure the approximation quality, TPPAA constructs the approximate function in monotonic form when the first order derivatives of two successive design points have the same signs, and vice versa. Moreover, when the monotonic form is required, the piecewise function is constructed to avoid the inappropriate approximation that the existing approximation methods may cause.

(2) To verify the practicability of TPPAA, a C++ program for structural optimization integrating CAD software, FEA software, approximation theory, and mathematical optimization method is developed.

(3) The performance of TPPAA is examined in several small scale structures and compared with other approximation methods. The result indicates that the structure optimization process is efficient by using TPPAA.

6.2   Suggestion

Here are two suggestions for further studies relevant to this research.

(1) Several studies have proposed some strategies for the determination of move limit

for each design variable according to specific information such as sensitivity. However, in this study, all the design variables have the same strategy of move limit which does not depend on any information. The improved strategies should be studied and applied to the SAO to make the process more stable.
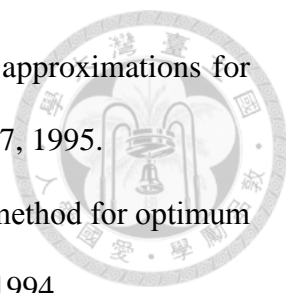
(2) In this study, the approximation methods are only applied to represent the stress, displacement in linear static analysis and natural frequency. The approximation methods can be tested further with other kinds of structural behavior.
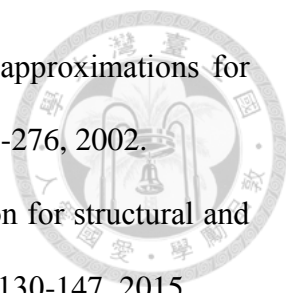
REFERENCES

[1] A. G. M. Mitchell, "The limits of economy of material in framed structures," Phil. Mag., series 6, 8, pp.589-597, 1904.

[2] L. A. Schmit and B. Farshi, "Some approximation concepts for structural synthesis," AIAA Journal, Vol.12, No.5, pp.692-699, 1974.

[3] K. Noor and H. E. Lowder, "Structural reanalysis via a mix method," Computers and Structures, Vol.5, pp.9-12, 1975.

[4] R. T. Haftka and C. P. Shore, "Approximation method for combined thermal structural design," NASA TP-1428, 1979.

[5] J. H. Starnes and R. T. Haftka, "Preliminary design of composite wings for buckling, strength, and displacement constraints," Journal of Aircraft, Vol.16, No.8, pp.564-570, 1979.

[6] C. Fleury and V. Brabaint, "Structural optimization : a new dual method using mixed variables," Int. J. Num. Meth. Engrg., Vol.23, pp.409-428, 1986.

[7] K. Svanberg, "The method of moving asymptotes-a new method for structural optimization," Int. J. Num. Meth. Engrg., Vol.24, pp.359-373, 1987.

[8] R. T. Haftka, J. A. Nachlas, L. T. Watson, T. Rizzo and R. Desai, "Two-point constraint approximation in structural optimization," Computer methods in applied mechanics and engineering, Vol.60, pp.289-301, 1987.

[9] G. M. Fadel, M. F. Riley and J. M. Barthelemy, "Two-point exponential approximation method for structural optimization," Structural Optimization, Vol.2, pp.117-124, 1990.

[10] L. P. Wang and R. V. Grandhi, "Efficient safety index calculation for structural reliability analysis," Computers and Structures, Vol.52, No.1, pp.103-111, 1994.

[11] L. P. Wang and R. V. Grandhi, "Improved two-point function approximations for design optimization," AIAA Journal, Vol.33, No.9, pp.1720-1727, 1995.

[12] J. A. Snyman and N. Stander, "New successive approximation method for optimum structural design," AIAA Journal, Vol.32, No.6, pp.1310-1315, 1994.

[13] C. Fleury and W. H. Zhang, "Selection of appropriate approximation schemes in multi-disciplinary engineering optimization," Advances in Engineering Software, Vol.31, No.6, pp.385-389, 1995.

[14] W. H. Zhang and C. Fleury, "A modification of convex approximation methods for structural optimization," Computers and Structures, Vol.64, No.1, pp.89-95, 1997.

[15] S. Xu and R. V. Grandhi, "Effective two-point function approximation for design optimization," AIAA Journal, Vol.36, No.12, pp.2269-2275, 1998.

[16] G. Xu, K. Yamazaki and G. D. Cheng, "A new two-point approximation approach for structural optimization," Struct Multidisc Optim, Vol.20, pp.22-28, 2000.

[17] M. S. Kim, J. R. Kim, J. Y. Jeon and D. H. Choi, "Efficient mechanical system optimization using two-point diagonal quadratic approximation in the nonlinear intervening variable space," KSME International Journal, Vol.15, No.9, pp.1257-1267, 2001.

[18] H. Chickermane and H. C. Gea, "Structural optimization using a new local approximation method," International Journal for Numerical Methods in Engineer, Vol.39, pp.829-846, 1996.

[19] A. A. Groenwold, L. F. P. Etman, J. A. Snyman and J. E. Rooda, "Incomplete series expansion for function approximation," Structural and Multidisciplinary Optimization, Vol.34, No.1, pp.21-40, 2007.

[20] C. Zillober, "A globally convergent version of the method of moving asymptotes," Structural Optimization, Vol. 6, pp.166-174, 1993.

[21] M. Bruyneel, P. Duysinx and C. Fleury, "A family of MMA approximations for structural optimization," Struct Multidisc Optim, Vol.24, pp.263-276, 2002.

[22] L. Li and K. Khandelwal, "An adaptive quadratic approximation for structural and topology optimization," Computers and Structures, Vol.151, pp.130-147, 2015.

[23] 邱求慧, 結構最佳設計保守近似法之改良, 台大機械工程學研究所博士論文, 2000.

[24] 陳建元, 兩點近似法於結構最佳化設計之應用, 台大機械工程學研究所碩士論文, 2002.

[25] 張耀仁, 結構最佳化設計之準二次兩點保守近似法, 台大機械工程學研究所碩士論文, 2007.

[26] 陳奕璋, 結構最佳化之指數移動漸進線近似法, 台大機械工程學研究所碩士論文, 2010.

[27] 陳俊傑, 結構最佳化之新式混合兩點近似法. 台大機械工程學研究所碩士論文, 2012.

[28] 江奇鴻, 結構最佳化之加強兩點指數近似法. 台大機械工程學研究所碩士論文, 2013.

[29] 王栢村, 環境振動試驗用印刷電路板之模型驗證, 中華民國力學學會第二十九屆全國力學會議, 新竹市, 2005.

[30] R, F, Gibson, "Modal vibration response measurements for characterization of composite materials and structures," Composite Science and Technology, Vol.60, No.15, pp.2769-2780, 2000.

Appendix: User manual of integrated optimization program

The optimization program for this research is developed in Microsoft Visual Studio 2015 with integrating AutoCAD and ANSYS. The instructions of this program are shown in this appendix.

A.1 Program setting

Important program settings are shown as follows. (Take 3-bar truss optimization as the example)

(a) Setting the path of AutoCAD and ANSYS (main.cpp)

```
// path of AutoCAD
acad_bat("D:\\Autodesk\\AutoCAD 2015\\acad.exe");
// path of ANSYS
ansys_bat("D:\\ANSYSInc\\v150\\ANSYS\\bin\\winx64\\ansys150.exe");
```

(b) Defining the optimization problem (main.cpp)

```
// set the number of the total functions and design variables respectively
DesignPoint point0(1 + 3, 2);
// initial design vector
point0 = { 2,1 };
// number of behavior constriants
Constraint design_constraint(point0.num_func - 1);
// upper bound and lower bound of each behavior constraint
design_constraint.make_behavior({ { -15.0,20.0 },{ -15.0,20.0 },{ -15.0,20.0 } });
```

(c) Selecting of the algorithms (main.cpp)

```
// Choose the approximation and optimization methods
    Approximation* pApprox1 = new ConvexLinear;
    Approximation* pApprox2 = new TPPAA(2, -2, 0.001, 0.001);
  ConstraintElimination* pCE = new ExteriorPenalty3(10, 1);
   SearchDirection* pSD = new BFGS;
   RangeFinder* pRF = new RangeFinder1;
   MinimumLocator* pML = new GoldenSection;
```

77

(d) Integration with AutoCAD and ANSYS (main.cpp)

```
// Whether modeling by AutoCAD
    bool run_cad = false;
    // the .lsp file name and the drawing function name for AutoCAD
    if (run_cad) // Lisp file name and the function name
        autocad_fileout(point0, "drawplate.lsp", "plate");
    // the .mac file name for ANSYS
    ansys_fileout(point0, "TS03.MAC");
```
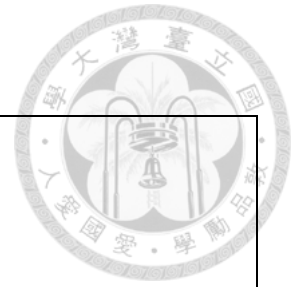
(e) Constraint treatment (main.cpp)

```
for (int i = 0; i < point0.num_func - 1; i++) {
    if (point0.value.component[i + 1] >= 0.0)
        treat.value.component[i + 1] /=design_constraint.behavior[i].second.component[0];
    else
        treat.value.component[i + 1] /= design_constraint.behavior[i].first.component[0];
    treat.value[i + 1] -= 1.0;

    for (int j = 0; j < point0.num_var; j++) {
        if (point0.value.component[i + 1] >= 0.0)
            treat.sensitivity[i + 1][j] /= design_constraint.behavior[i].second.component[0];
        else
            treat.sensitivity[i + 1][j] /= design_constraint.behavior[i].first.component[0];
    }
}
```

(f) Move limit (main.cpp)

```
// move limit definition
for (int i = 0; i < point0.num_var; i++)
    move_limit[i] = { point0.variable.component[i] / 3.0 , point0.variable.component[i] * 3.0 };
```

(g) Defining the explicit objective function (Approximation.h)

```
#define explicit_objective {\
if (index_func_nf == 0) {\
    value = 20 * sqrt(2) * x(0) + 10 * x(1);\
    return *this;\
}\
}
#define explicit_objective_gradient {\
if (index_func_nf==0){\
    grad(0) = 20 * sqrt(2);\
    grad(1) = 10.0;\
    return *this;\
}\
}
#endif
```

78

A.2 Operation step

Operation steps of the program are listed in the following and shown in Fig. A-1.

(1) Open "ThreeBarTruss.vcxproj".

(2) Open "main.cpp".

(3) Set the program as in section A-1.

(4) Press "Ctrl+F5".

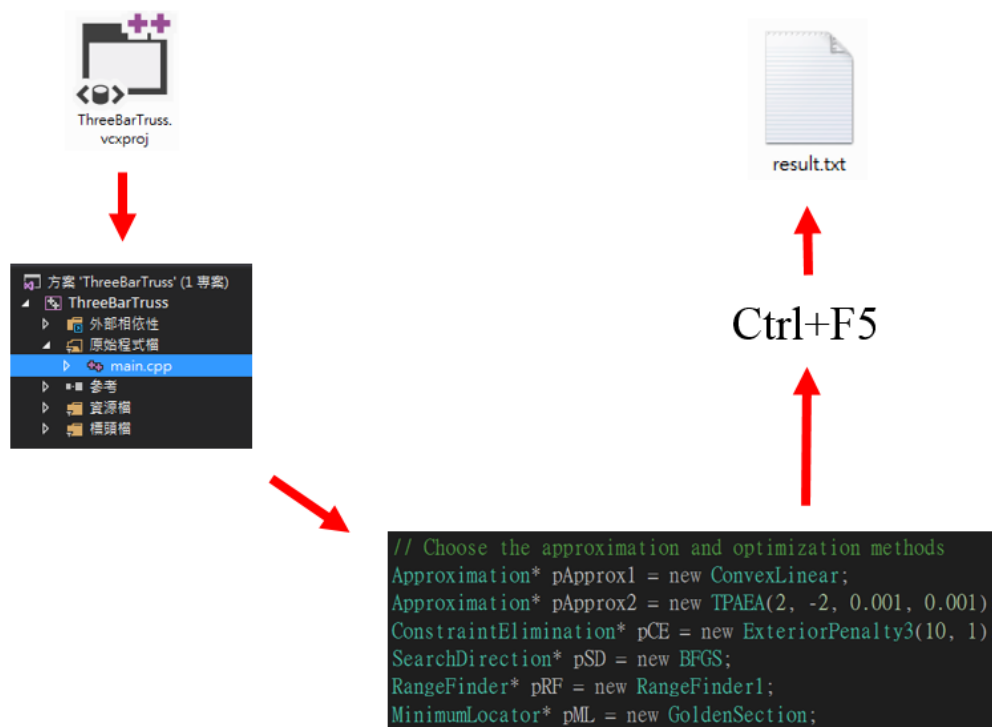(5) The result is recorded in "result.txt"

Fig. A-1 Operation steps of the optimization program

79

Vitae

Name: Hao-Yu Ke 柯浩宇

Date of birth: August 25, 1992

Phone: 0989-742056

E-mail: r03522633@ntu.edu.tw

Educational background:

1998-2004   Taichung City Wuchi Elementary School

臺中市立梧棲國民小學

2004-2007   Taichung City Wuchi Junior High School

臺中市立梧棲國民中學

2007-2010   National Taichung First Senior High School

國立臺中第一高級中學

2010-2014   Department of Mechanical Engineering, National Cheng Kung University

國立成功大學機械工程學系

2014-2016   Institute of Mechanical Engineering, National Taiwan University

國立臺灣大學機械工程學研究所